QEX
$5
September/October 2011
www.arrl.org

A Forum for Communications Experimenters

Issue No. 268

W2FS uses a pair of XBee Pro transceivers to build USB and serial communications modules. This virtual serial cable (VSC-X) can be used to program a radio or for a variety of other applications where you want a serial communications link without wires.

ARRL The national association for AMATEUR RADIO™
225 Main Street
Newington, CT USA 06111-1494

HF/50MHz ALL MODE TRANSCEIVER TS-590

Nothing But Performance

The TS-590S

Kenwood has essentially redefined HF performance with the TS-590S compact HF transceiver. The TS-590S RX section sports IMD (intermodulation distortion) characteristics that are on par with those "top of the line" transceivers, not to mention having the best dynamic range in its class when handling unwanted, adjacent off-frequency signals.*

- **HF-50MHz 100W**
- **Digital IF Filters**
- **Built-in Antenna Tuner**
- **Advanced DSP from the IF stage forward**
- **Heavy duty TX section**
- **500Hz and 2.7KHz roofing filters included**
- **2 Color LCD**

KENWOOD
Listen to the Future

www.kenwoodusa.com

KENWOOD U.S.A. CORPORATION
Communications Sector Headquarters
3970 Johns Creek Court, Suite 100, Suwanee, GA 30024
Customer Support/Distribution
P.O. Box 22745, 2201 East Dominguez St., Long Beach, CA 90801-5745
ADS#13211 Customer Support: (310) 639-4200 Fax: (310) 537-8235

* For 1.8/3.5/7/14/21 MHz Amateur bands, when receiving in CW/FSK/SSB modes, down conversion is automatically selected if the final passband is 2.7KHz or less.

QEX (ISSN: 0886-8093) is published bimonthly in January, March, May, July, September, and November by the American Radio Relay League, 225 Main Street, Newington, CT 06111-1494. Periodicals postage paid at Hartford, CT and at additional mailing offices.

POSTMASTER: Send address changes to: QEX, 225 Main St, Newington, CT 06111-1494
Issue No 268

Harold Kramer, WJ1B
Publisher

Larry Wolfgang, WR1B
Editor

Lori Weinberg, KB1EIB
Assistant Editor

Zack Lau, W1VT
Ray Mack, W5IFS
Contributing Editors

Production Department

Steve Ford, WB8IMY
Publications Manager

Michelle Bloom, WB1ENT
Production Supervisor

Sue Fagan, KB1OKW
Graphic Design Supervisor

David Pingree, N1NAS
Senior Technical Illustrator

Carol Michaud, KB1QAW
Technical Illustrator

Advertising Information Contact:

Janet L. Rocco, W1JLR
Business Services
860-594-0203 – Direct
800-243-7768 – ARRL
860-594-4285 – Fax

Circulation Department

Cathy Stepina, *QEX Circulation*

Offices

225 Main St, Newington, CT 06111-1494 USA
Telephone: 860-594-0200
Fax: 860-594-0259 (24 hour direct line)
e-mail: **qex@arrl.org**

Subscription rate for 6 issues:

In the US: ARRL Member $24, nonmember $36;

US by First Class Mail:
ARRL member $37, nonmember $49;

International and Canada by Airmail: ARRL member $31, nonmember $43;

Members are asked to include their membership control number or a label from their QST when applying.

In order to ensure prompt delivery, we ask that you periodically check the address information on your mailing label. If you find any inaccuracies, please contact the Circulation Department immediately. Thank you for your assistance.

About the Cover

John Hansen, W2FS, describes how he uses a pair of XBee Pro transceivers to build USB and serial communications modules that create a virtual serial cable (VSC-X). The VSC-X gives you a serial communications link without wires. Program your radio remotely or use it for other applications where you don't want to be tethered to your computer.

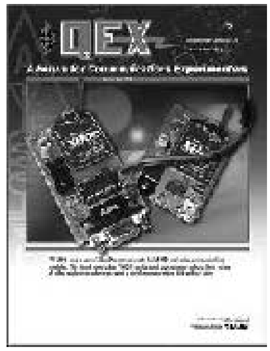

In This Issue

Features

Index of Advertisers

The American Radio Relay League

The American Radio Relay League, Inc, is a noncommercial association of radio amateurs, organized for the promotion of interest in Amateur Radio communication and experimentation, for the establishment of networks to provide communications in the event of disasters or other emergencies, for the advancement of the radio art and of the public welfare, for the representation of the radio amateur in legislative matters, and for the maintenance of fraternalism and a high standard of conduct.

ARRL is an incorporated association without capital stock chartered under the laws of the state of Connecticut, and is an exempt organization under Section 501(c)(3) of the Internal Revenue Code of 1986. Its affairs are governed by a Board of Directors, whose voting members are elected every three years by the general membership. The officers are elected or appointed by the Directors. The League is noncommercial, and no one who could gain financially from the shaping of its affairs is eligible for membership on its Board.

"Of, by, and for the radio amateur," ARRL numbers within its ranks the vast majority of active amateurs in the nation and has a proud history of achievement as the standard-bearer in amateur affairs.

A *bona fide* interest in Amateur Radio is the only essential qualification of membership; an Amateur Radio license is not a prerequisite, although full voting membership is granted only to licensed amateurs in the US.

Membership inquiries and general correspondence should be addressed to the administrative headquarters:

ARRL
225 Main Street
Newington, CT 06111 USA
Telephone: 860-594-0200
FAX: 860-594-0259 (24-hour direct line)

Officers

President: KAY C. CRAIGIE, N3KN
570 Brush Mountain Rd, Blacksburg, VA 24060

Chief Executive Officer: DAVID SUMNER, K1ZZ

The purpose of *QEX* is to:

1) provide a medium for the exchange of ideas and information among Amateur Radio experimenters,

2) document advanced technical work in the Amateur Radio field, and

3) support efforts to advance the state of the Amateur Radio art.

All correspondence concerning *QEX* should be addressed to the American Radio Relay League, 225 Main Street, Newington, CT 06111 USA. Envelopes containing manuscripts and letters for publication in *QEX* should be marked Editor, *QEX*.

Both theoretical and practical technical articles are welcomed. Manuscripts should be submitted in word-processor format, if possible. We can redraw any figures as long as their content is clear. Photos should be glossy, color or black-and-white prints of at least the size they are to appear in *QEX* or high-resolution digital images (300 dots per inch or higher at the printed size). Further information for authors can be found on the Web at **www.arrl.org/qex/** or by e-mail to **qex@arrl.org**.

Larry Wolfgang, WR1B

Empirical Outlook

We've Got e-Mail

One of the "advantages" of being the Editor of *QEX* is that I get on all kinds of e-mail lists, without even asking! Rarely does a day go by when my in-box isn't flooded with news releases, offers of "free" articles for publication and other things you can't even imagine. Most of it has nothing to do with who we are at ARRL and *QEX*. No, my readers would not be interested in the latest press release about an organization's political agenda, announcements about a company's new CEO, the latest society news or just about anything else these lists have to offer. Of course trying to unsubscribe from the list just confirms that they have a valid e-mail address, and redoubles their efforts to send annoying spam!

Most of the time I don't need to read the first line of the text to know I can just hit the "Delete" button. Every once in a while a headline catches my eye, though, and I read a few lines, out of curiosity. Some of the more interesting e-mails are offers of "free articles" being offered for publication. Most of these stories appear to be promoting some author's new book, lecture tour or perhaps a webinar to join. Of course the actual information is never included. If you want that, you'll have to contact the promoter or log on to some website.

On rare occasions, one of these e-mails actually leads to some interesting information. A couple of weeks ago there was a notice about a FEMA IPAWS webinar with regard to a nationwide test of the emergency alert system (EAS). Most of us recognize the FEMA acronym, but I had never heard of IPAWS. Something for the dogs? Apparently not. Part of the notice read:

"You're invited by the FEMA Integrated Public Alert and Warning System (IPAWS), Federal Communications Commission (FCC), National Oceanic and Atmospheric Administration (NOAA), and industry experts to the next EAS Participant Virtual Roundtable: Are You Ready for the Nationwide EAS Test?

"In order to prepare EAS Participants for the November 9, 2011 Nationwide EAS Test, FEMA IPAWS, the FCC, and NOAA are partnering with industry leaders and experts to draft a comprehensive technical best practices guide on end-to-end National EAS message procedures. The guide will be updated incrementally with the EAS community through webinars, roundtables, and other activities leading up to the Test.

"For more information on the Nationwide EAS Test, please visit the **FEMA IPAWS** website: **www.fema.gov/emergency/ipaws/eas_info.shtm."**

Since we, as Amateur Radio operators, are very interested in emergency communications, I thought this might be of interest. I missed the original webinar, but I intend to learn more about this nationwide test. I realize that Amateur Radio operators aren't involved with the emergency broadcast system, but in a real emergency, we could quickly become involved in communications activity!

Of course I do also receive e-mails from groups that I have signed up with, or which come in and turn out to often be of interest. Several electronics manufacturers fall into this category. I normally glance through the announcements from National Semiconductor, just to see what might be of interest. When I saw the newsletter about their new RF direct sampling analog to digital converters, I wanted to learn more:

"The industry's first direct RF-sampling ADC directly samples input frequencies beyond 2.7 GHz at up to 3.6 GSPS with excellent dynamic performance. The ADC12Dxx00RF replaces multiple analog components with a single chip, allowing radio designers to increase system capacity and flexibility while reducing board size, weight, and cost and simplifying the design process. A wide range of applications such as 3G/4G wireless base stations, microwave backhaul, military, and wideband software-defined radio (SDR) can now achieve the benefits that RF-sampling provides."

Check out the National website for more information. (**www.national.com/pf/DC/ADC12D1800RF.html#Overview**) I didn't find any pricing information, although I imagine that at this stage they are well beyond the reach of any casual Amateur Radio project. Still, we can dream, can't we? Perhaps some of our readers have already sampled these devices and have a circuit working on the evaluation board. Can you tell us about it? I'm sure many readers would be quite interested in even some preliminary data about these new ICs.

If you haven't browsed the National website in a while, it is a good one to check out from time to time. They offer a variety of free downloads, including various *Spice* simulation models and their "Webench Designer" programs. Other manufacturers also offer plenty of information to

(Continued on page 7)

John A. Hansen W2FS

49 Maple Avenue, Fredonia, NY 14063; john@coastalchip.com

VSC-X: A Virtual Serial Cable to Remotely Program Your Mobile Radio

How long of a serial cable do you *need? Transfer your data wirelessly!*

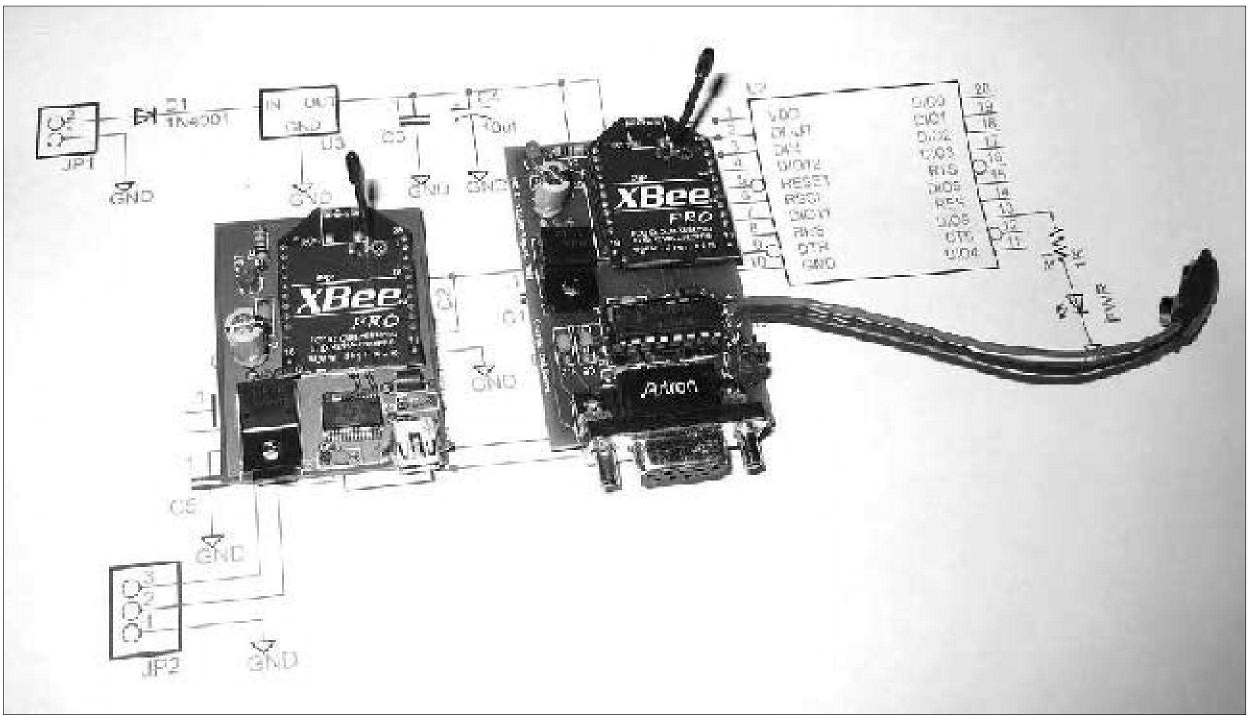

With hundreds if not thousands of memories available, mobile radios have become increasingly capable and increasingly complex to program. This has naturally given rise to the development of computer software to allow users to manage memory contents and program the radios. Mobile radios, however, are most often located in cars and trucks where users generally don't have computers. As a result, in order to program the radios it is necessary to either bring the radio inside to a computer or bring a computer to the radio. This inconvenience means that many users make changes to their radios either infrequently, or never.

Every ham radio operator knows that the solution to transmitting data over a distance that is too long for a cable run is, of course, radio. Using radio to program your mobile *radio*, however, requires that you find something faster and more robust than the standard 1200 baud (or even 9600 baud) packet signals that most hams think of when they think about data transfer over radio. A lot of software for programming radios requires that the effective data throughput (not just the raw bit rate) be at least 9600 bits per second.

There are some higher speed digital radio links available, but for the most part they are *very* low power or *very* expensive. What we need is an inexpensive way to transmit data with at least a 9600 bit per second throughput that has a signal strong enough to provide reliable communications between a computer in the house and a mobile radio inside a car. It would also be nice if the resulting data link

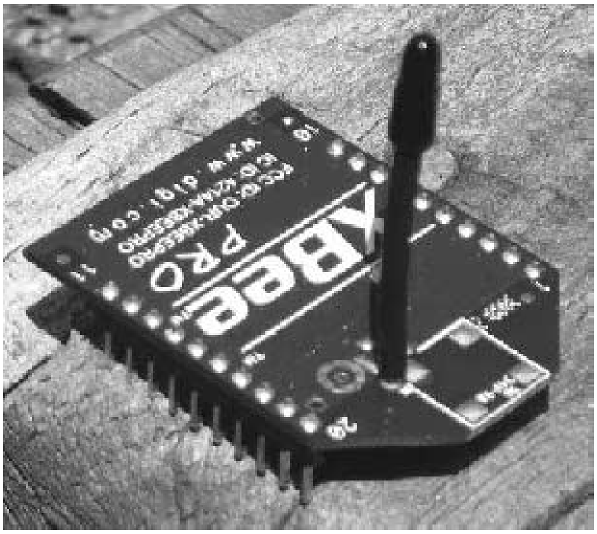

Figure 1 — The XBee-Pro module (wire antenna version).

could use a USB port on the computer rather than the rapidly vanishing serial port. Finally, it would be nice if this serial link could work for both radios that have conventional RS-232 serial ports (such as the Kenwood D700 and D710) and radios that have TTL level serial ports (such as most ICOM and Yaesu radios). The virtual serial cable (VSC-X) described in this article provides exactly this solution.

A company called Digi, Inc. manufactures a line of data transceivers called XBee modules. These modules provide a transparent data link that is capable of continuous throughput of at least 9600 bits per second. The modules come in two power levels. The XBee Pro module is most useful for this project, because the output power of the unit is 50 mW. This is substantially higher than the 1 to 2 mW that is available on most inexpensive RF data modules. The XBee Pro modules are available in three antenna configurations. You can get them with an on-board "chip" antenna, but somewhat better range can be had with what they call a "wire" antenna. This is essentially a tiny whip (see Figure 1). Alternatively, it is also possible to purchase these modules with a U.Fl antenna connector in order to connect a range of other antennas. The radios operate in the popular 2.4 GHz frequency band. The price of the XBee Pro module is only about $32 each from Digi-Key, Mouser and other suppliers.

The XBee modules use the ZigBee protocol. Wikipedia describes ZigBee as a specification for a suite of high level communication protocols using small, low-power digital radios based on an IEEE 802.15.4 standard for personal area networks.

The data interface to the modules is asynchronous serial TTL level data. As a result, it

(A)

(B)

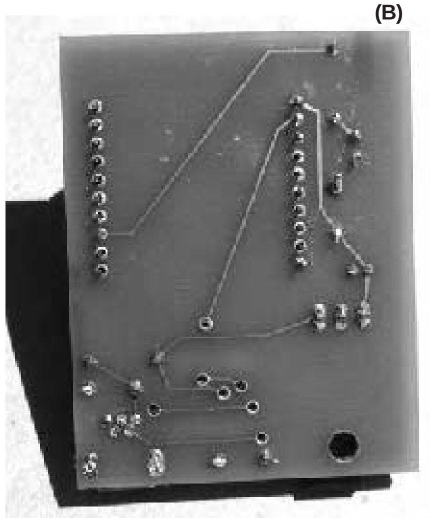

Figure 2 — The VSC-X USB adapter is shown here. Part A is the top of the circuit board and Part B is the bottom of the board.

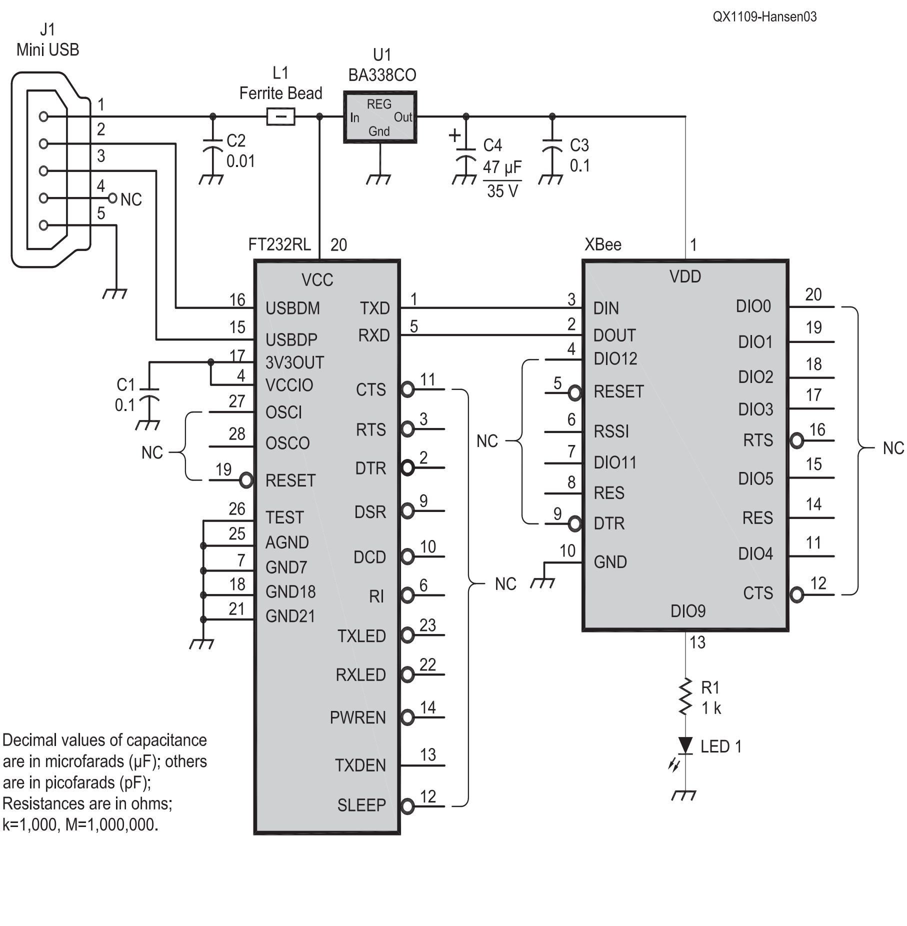

Figure 3 — VSC-X USB adapter circuit.

is relatively easy to interface them to either a PC (assuming you provide a USB or RS232 interface) or to a radio (with no interface for radios that support TTL level signals or with an RS232 level converting interface for the rest). In either case it's not really necessary to provide any "intelligence" in the circuit beyond that which is supplied by the XBee module itself. The XBee module also requires a 3.3 V power supply of approximately 300 mA.

Casual experimentation showed that the XBee-Pro modules could easily handle 9600 bps data over fairly decent distances. I plugged one into the computer on the second floor of my house and was able to walk 3 houses down the street with no loss of data. I brought the unit back to my driveway, put it in the trunk of my car and closed the trunk and still had almost perfect copy. With the radio on the floor of my car under the driver's seat and the car parked in the driveway with the doors closed, I had no trouble reprogramming the radio from inside the house. Digi's documentation says the units have an outdoors range of up to a mile, but I tend to discount manufacturer range claims (perhaps they were using the model that could connect to an external antenna). Of course, your mileage may vary.

I wanted to create modules that would provide all of the circuitry necessary to interface the XBee modules to a computer and to a remote radio. I've called the resulting adapter pair VSC-X, meant to describe an eXtended Virtual Serial Cable.[1] On the PC side, this involves creating a USB interface. Power for the VSC-X USB module is drawn directly from the USB port on the computer, but a 3.3 V regulator is required to step down the 5 V USB power supply to 3.3 V. See Figure 2. The USB interface to the computer is provided by a standard FTDI FT232RL USB interface chip. The resulting circuit is shown in Figure 3. Note: C4 must be at least 35 V.

To use the VSC-X USB adapter, you first must load a driver on your computer. Drivers are available for Windows and Mac OS operating systems on the FTDI driver website: **www.ftdichip.com/Drivers/VCP.htm**.

If you are using *Linux*, the driver is already built into the kernel. After the driver is installed, when you plug the VSC-X adapter into your computer (using a mini USB cable such as those that usually come with digital cameras) the adapter will appear as a serial port on your computer. If you prefer that it be a different COM port designation (for example, if the COM port number is too high to be recognized by your radio programming software), you can change this from the Windows Device Manager.

I developed a second board to support the serial port connection to the mobile radio. The VSC-X serial adapter requires 5 to 15 V dc at 300 mA. Typically this would be provided either by the radio power supply or with a 9 V battery. Be very careful if you power it from the radio power supply, because if the ground connection from the adapter to the power supply comes loose, the full 300 mA will flow through the ground circuit on the radio's computer connector. See Figure 4. The VSC-X adapter reduces the input voltage to 3.3 V to power the XBee module. The XBee module also uses 3.3 V signal levels. As a result, I used the 3 V version of the usual MAX 232 chip (the ICL3232). The resulting circuit is shown in Figure 5. Note: C4 must be at least 35 V. (This may have more to do with the need for a low equivalent series resistance (ESR) rating than it does with the voltage rating, but 35 V and higher capacitors have worked reliably in the circuit.)

The VSC-X serial adapter uses a female DB-9 connector. Since radios that use RS-232 level signals (like the Kenwood D700) generally have male DB-9 connectors, the adapter will plug directly into the radio (no cable required!). While the Kenwood D710 also uses RS-232 level signals, it does not have a DB-9 connector. As a result, an adapter cable is necessary to connect to the radio's 8 pin mini-DIN connector. You can either use the PG-5G cable available from Kenwood, or you can construct your own using the diagram in Figure 6. (The PG-5G cable uses a female DB-9 connector, so you will need a "gender changer" adapter with that cable.)

If the radio you are using requires TTL level signals rather than RS232 level signals (for example, the Yaesu FT-857 or most ICOM radios), it is necessary to remove the ICL3232 from its socket and jumper the inputs and outputs of the chip's socket. This is done by placing jumpers across pins 1 and 2 and across pins 3 and 4 of JP1.

Since virtually all radios that use TTL level signals do not have a DB-9 connector, it will be necessary to construct a cable that connects the TXData, RXData and ground lines. For example, on the 800 series Yaesu radios, the connection to the computer is made through an 8 pin mini-DIN connector, wired as shown in Figure 7.

In order to connect VSC-X to an ICOM

[1]Notes appear on page 7.

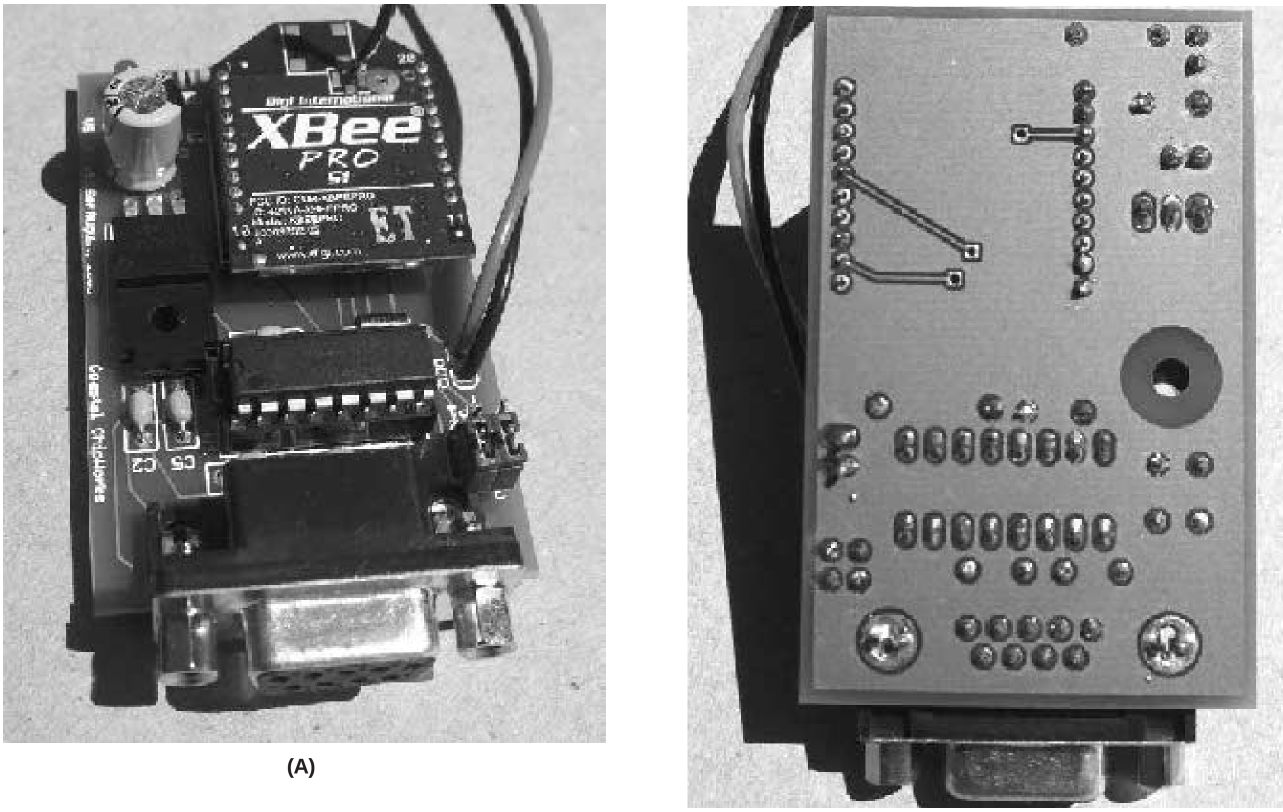

(A)

(B)

Figure 4 — The VSC-X serial adapter is shown in this photo. Part A is the top of the circuit board and Part B is the bottom of the board.

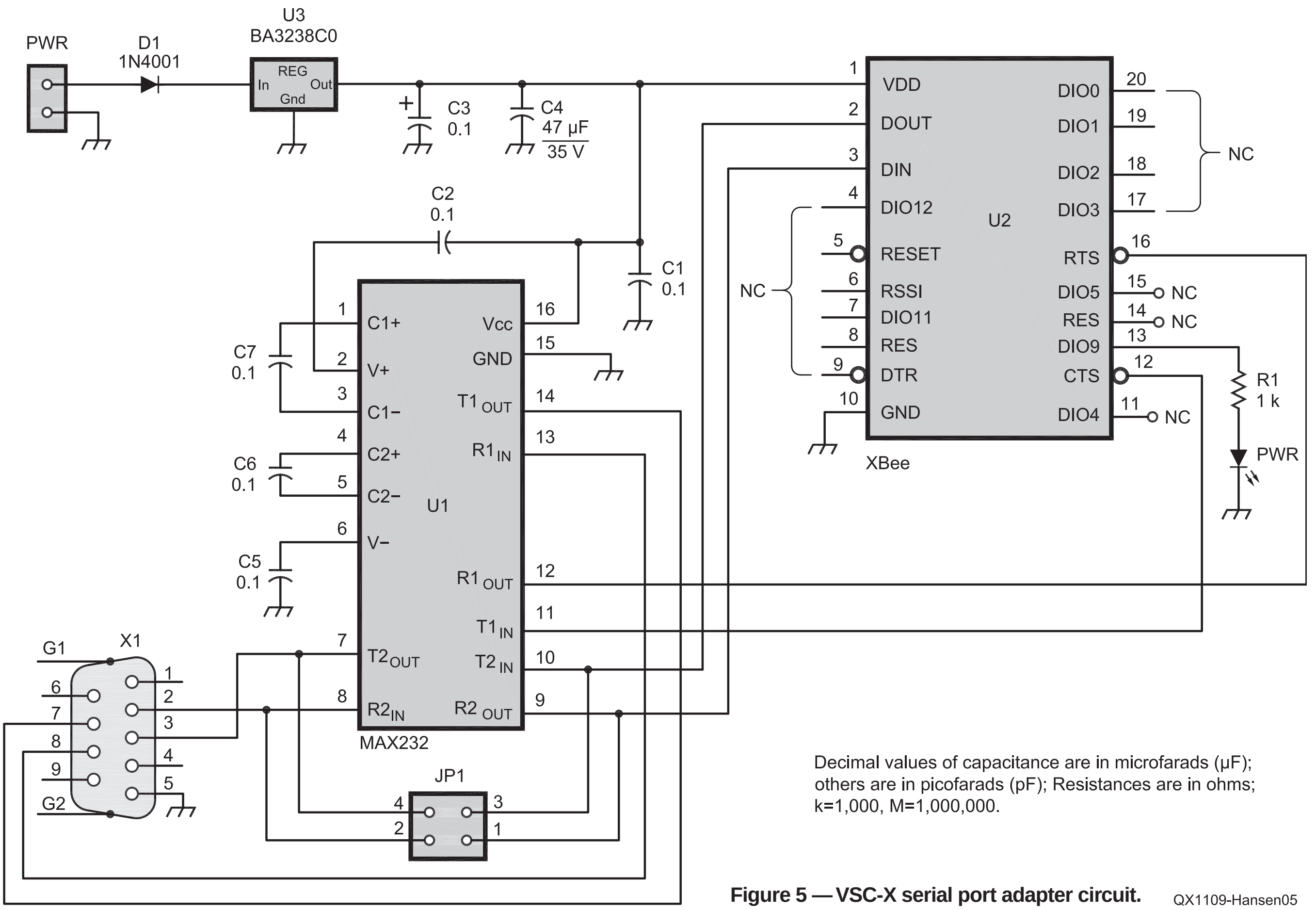

Figure 5 — VSC-X serial port adapter circuit. QX1109-Hansen05

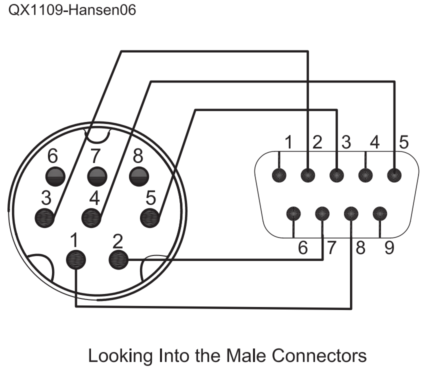

Figure 6 — A wiring diagram for connecting VSC-X to a Kenwood TM-D710 transceiver.

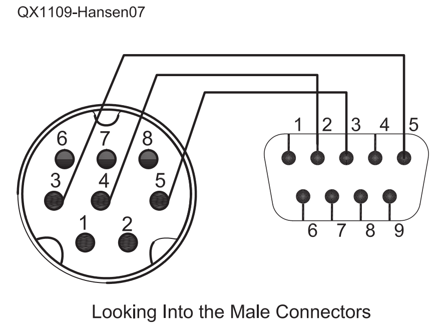

Figure 7 — A wiring diagram for Yaesu 800 series radios such as the FT817, FT857, FT897 and other radios.

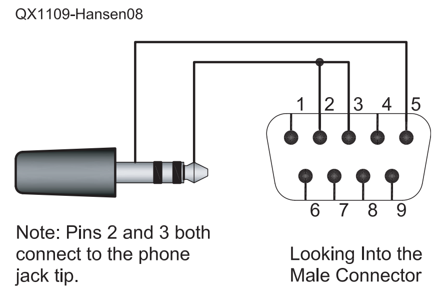

Figure 8 — This wiring diagram is for ICOM radios that use a CI-V style interface.

radio with a CI-V interface (IC-706, IC-756, IC-703 and others), you will need an adapter using a ⅛ inch phone plug using the wiring diagram shown in Figure 8.

Using the VSC-X modules is fairly straightforward. There is nothing that requires configuration; you just plug them in and they work. Configure your radio programming software to use the port where the USB module appears after driver installation, and set the data rate to 9600 baud and you should be ready to program your radio.

While the VSC-X was designed to allow remote reprogramming of mobile radios, it can be used for virtually any application where a serial port connection is needed and data flows at a rate of 9600 baud or less. Remote antenna tuners that are controlled by serial ports or weather stations that deliver data over a serial connection are two examples of other applications that have been suggested for VSC-X. You might have other ideas for ways to use your virtual serial cable. [How about a connection between two computers to transfer files? Your editor is considering a pair as a way to put his old West Mountain Radio RigBlaster back into service with a computer that lacks the required serial port. What other applications can you come up with?—*Ed.*]

Notes

[1]A complete set of boards and all of the parts necessary to build a pair of VSC-X modules (except the XBee Radios) is available for $40 plus $5 shipping from John A. Hansen, 49 Maple Avenue, Fredonia, NY 14063. A complete set of parts to build a pair of VSC-X modules, including 2 XBee Pro modules with whip antennas are available for $110 plus $8 shipping. Pre-wired radio cables are also available. Because of export restrictions, the kit with XBee Pro modules is only available for shipment to addresses inside the US. See **www.vsc-x.com** for more details.

(Continued from page 2)

Empirical Outlook

help you plan your next project. As another example, Microchip (**www.microchip.com**) provides all kinds of information about their PIC microcontrollers. They also offer free downloads of their MPLAB Integrated Development Lab design software as well as *Spice* models of many components. I imagine many readers have a long list of manufacturer's websites that they like to visit.

I'll be attending the ARRL/TAPR DCC in Baltimore this year (Sep 16-18), and I hope to meet many readers (and perhaps recruit some new ones) at that time.

In the last two issues you read about my efforts to restore older missing files on our *QEX* files website. I have added a few more files, and currently have all of them through 2002 available. Please keep checking **www.arrl.org/qexfiles**, and I'll keep working on the project.

Next Issue in *QEX*

Dave Gordon-Smith, G3UUR, brings us another of his ever popular filter articles. This time he presents "The Design of Mixed-Coupling LC Bandpass Ladder Filters." He describes some design difficulties associated with wide bandwidth asymmetrical bandpass ladder filters, and then presents a simple procedure to accomplish the design of such filters. He presents calculations for the filter inductors and capacitors based on tables of design coefficients for various order filters.

Arch Doty, W7ACD

21370 SW McCormick Hill Rd, Hillsboro, OR 97123; **archd@aol.com**

The Effect of Soil Properties on the Performance of Antenna Radials

While conducting some other research on ground conductivity and radial systems, the author was interrupted by some heavy rains. Learn how that changed the direction of his experiments.

On October 25, 2010 a three day rainfall in Oregon ended with a total accumulation of almost 3 inches of precipitation. On that same date what had been a rather routine antenna test program abruptly ended, and a new, and potentially important, line of investigation started.

The results of the tests that day indicated that all of the reports on buried radials that have been written during the past 75 years should be reviewed, as they are probably incomplete, and may be misleading.

The generally accepted "Bible" of data on buried radials used with vertical antennas is the historic 1937 *IRE* paper by Brown, Lewis and Epstine.[1] This paper has been the basis for many research efforts, countless Amateur Radio and commercial antennas, and is even the basis for the current FCC requirements for buried ground systems for AM broadcasting stations.[2] This paper, and many that followed it provided comprehensive information — but forgot to consider one vital factor – the effect of Ground Conductivity/ Soil Resistivity on the performance of buried radials.

The extensive test program that I started on October 25, 2010 has clearly indicated that the electrical properties of soil can have a dramatic effect on the performance of buried radials, and *must* be considered in evaluating their performance.

Soil composition, moisture content and temperature all affect soil resistivity (and, of course, its inverse, ground conductivity) to a major degree. Data provided by the Federal Communications Commission shows that ground conductivity in the United States varies from 0.5 to 30 millisiemens/meter — in other words, the conductivity in one area may be 60 times that in another!

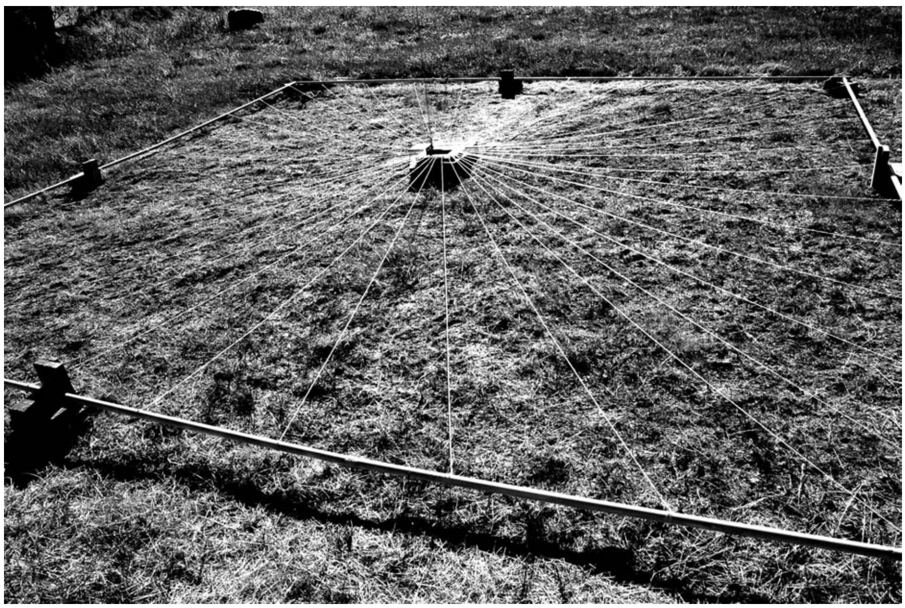

Figure 1 — This is a view of antenna number three, with 40 elevated radials.

The ongoing test program, which I fully described in the March/April 2011 issue of *QEX* was originally designed to determine whether elevated (counterpoise) or buried radials provided the best performance when used with ¼ λ vertical antennas.[3]

Three antennas were constructed. Each consisted of identical ¼ λ 10 meter verticals. The first antenna was located over a 20 by 20 foot ground system consisting of aluminum mesh. This was the "Standard" antenna that was to be used for comparison. The second antenna was identical, but was located over 40 radials, buried 4 inches below the surface, on a 20 by 20 foot square. The third antenna is identical to the others, but was at the center of 40 insulated radials elevated approximately 4 inches above ground level. See Figure 1. (This is equivalent to counterpoise radials elevated almost 5 feet under a 160 meter vertical).

More than 100 tests were made during, and at the end of, a typically beautiful Oregon Summer, which included eight weeks without a drop of rain. Those tests

[1]Notes appear on page 13.

conclusively showed that elevated radials provided an average of 1.18 dB more signal strength than did buried radials when they were used with ¼ λ vertical antennas. *Every* test showed the superiority of elevated radials.

It was then that we had almost 3 inches of rain, and, for the first time buried radials suddenly outperformed elevated ones! Tests made a few hours later, however, showed that the antenna systems had gone back to "normal," with elevated radials once again being superior.

In the following months there were 18 additional periods of heavy rain and, after *every one* of them, buried radials offered superior results for a short time. After one of these rains I made a series of tests and graphed the results. These graphs were made possible by using the unique software program, W8WWV's *S Meter Lite Software*, developed by Greg Ordy, W8WWV.[4] This program allows the small, notoriously inaccurate S meter on a receiver to be displayed as a calibrated signal strength bar graph, which on my computer is more than 9 inches long. The result is accuracy in reading signal strength that approaches 0.10 dB. A display of signal strength over an extended period of time is also provided. The plots shown in Figures 2 through 5 each cover a period of approximately five minutes, with the first half of the plot showing the performance of elevated radials, and the second half showing buried radials.

Figure 2 is a typical scan of what is always found when comparing two identical ¼ λ vertical antennas — one operating against 40 buried radials, the other with 40 identical, but elevated, radials — at any time that ground conductivity is normal, meaning there has not been any recent heavy rain.

Atmospheric Noise, which is predominantly vertically polarized, was used as a signal source in obtaining these traces. The left scale is in dB below the signal required to indicate "S-9" on a carefully calibrated communications receiver. "Squiggles" on the horizontal trace represent approximately 0.10 dB variations.

Immediately after a 0.72 inch rainfall I made a series of measurements and plotted that data in Figure 3. Note that in this graph, buried radials have a distinct advantage.

The graph of Figure 4 is a plot of data collected 60 minutes after that 0.72 inch rainfall. Elevated and buried radials now show about equal performance.

The next set of data was collected 150 minutes after the end of 0.72 inch rainfall. Elevated radials have begun to show better performance as the rain water continues to seep further into the earth, thus lowering the

QX1109-Doty02

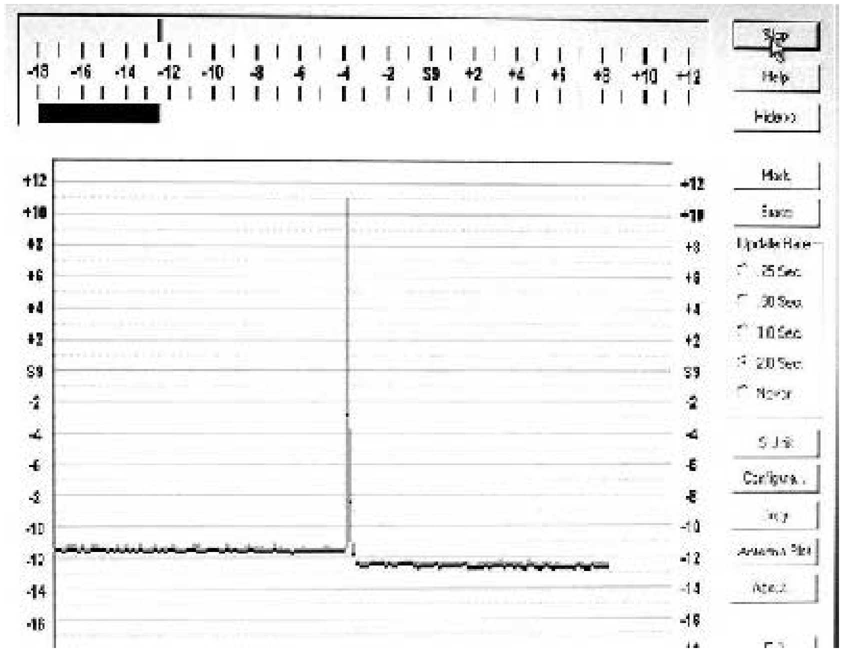

Figure 2 — This graph shows the "normal" relative performance of vertical antennas using elevated and buried radials. Signals from the elevated radials are displayed to the left of the main signal spike and signals from the buried radials are shown to the right of the signal spike.

QX1109-Doty03

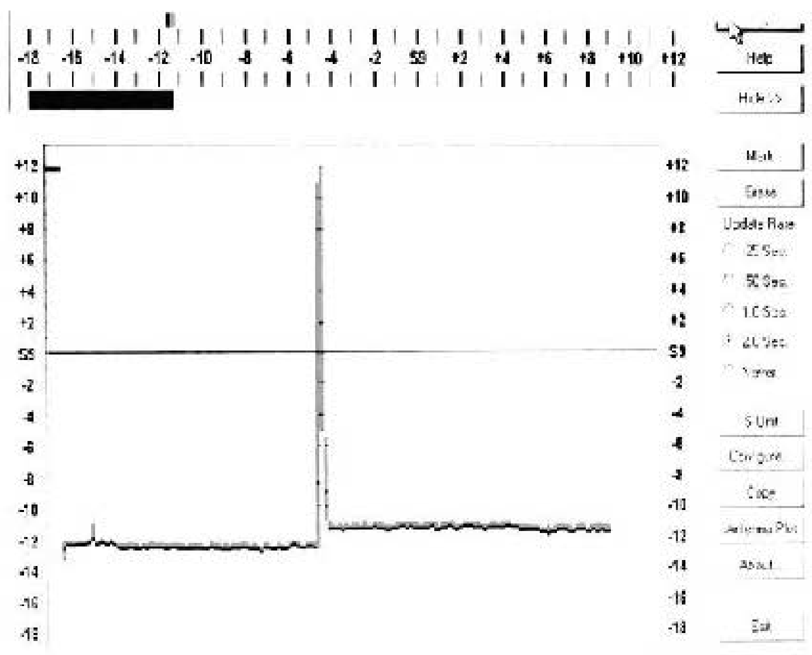

Figure 3 — I made these measurements immediately after the end of a 0.72 inch rainfall. Signals from the elevated radials are displayed to the left of the main signal spike and signals from the buried radials are shown to the right of the signal spike.

ground conductivity in the vicinity of the buried radials. Notice that the *SMeter* bar graph at the top of the chart is showing –11.9 dB in Figure 5 as compared to about –12.1 dB in Figure 4.

Methodology

To investigate the effect of moisture on the performance of buried radials it is necessary to be able to measure the electrical characteristics of the soil at the specific depths where the radials are located, and here there is a problem. For more than 20 years I have been using the method of measuring ground conductivity developed and published by Jerry Sevick in the March 1981 issue of *QST*.[5] Sevick's system was apparently based on the four-probe "Wenner Method" of measuring soil conductivity — the generally accepted method of making such measurements since it was created at the US Bureau of Standards in 1915.[6] Neither of these methods could be used in the current test program, however, because they both incorporate four ground probes — each one foot long. Thus they measure the *average* ground conductivity of the top foot (and more) of the soil, not just the top few inches, where the radials are located.

To solve this problem I built a test rig using 5 inch probes, in order to determine the changes that take place in the soil's electrical properties in the vicinity of the buried radials. The probes that I built are spaced 8.5 feet apart. This distance was established by a series of tests with the probes at various spacings, and then comparing the results with the readings on my Sevick array that is installed nearby.

Measurements were made with an Advance Devices "High Precision LCR Meter," which provided 1% accuracy of readings and was obtained exclusively for this test program.

As a matter of information, when the test site was first built, an eight foot ground rod was driven into the soil immediately adjacent to the elevated radials at antenna number three. During the test program, occasional readings were taken of the capacity between the radials and this ground. It was found that this capacity did vary with the variation in ground conductivity, with a corresponding slight change in the resonant frequency — a change that did not affect the performance of the antenna. A full description of this "Capacitive Bottom Loading" effect is available on my website.[7]

Discussion of Findings

As shown by the graphs presented previously, buried radials are superior to elevated ones immediately after heavy rain, but only

QX1109-Doty04

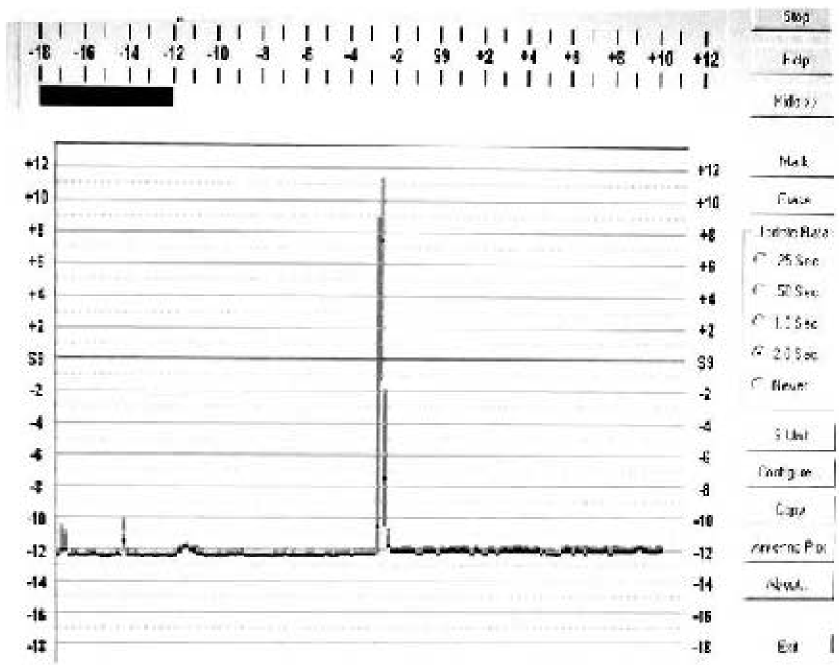

Figure 4 — The data for this graph was collected 60 minutes after the end of a 0.72 inch rainfall. Signals from the elevated radials are to the left and signals from the buried radials are to the right.

QX1109-Doty05

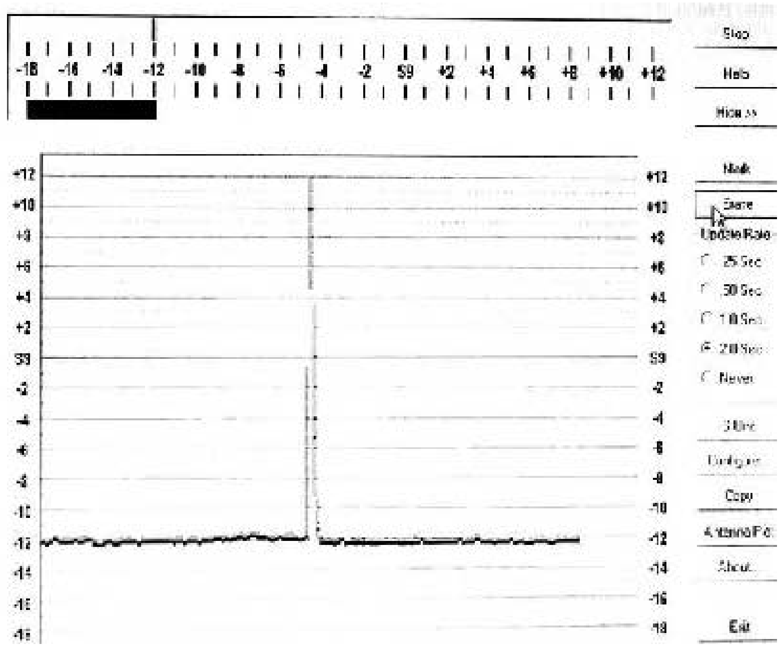

Figure 5 — At 150 minutes after the end of the 0.72 inch rainfall I made another set of measurements, with that data plotted here. Signals from the elevated radials are to the left and signals from the buried radials are to the right.

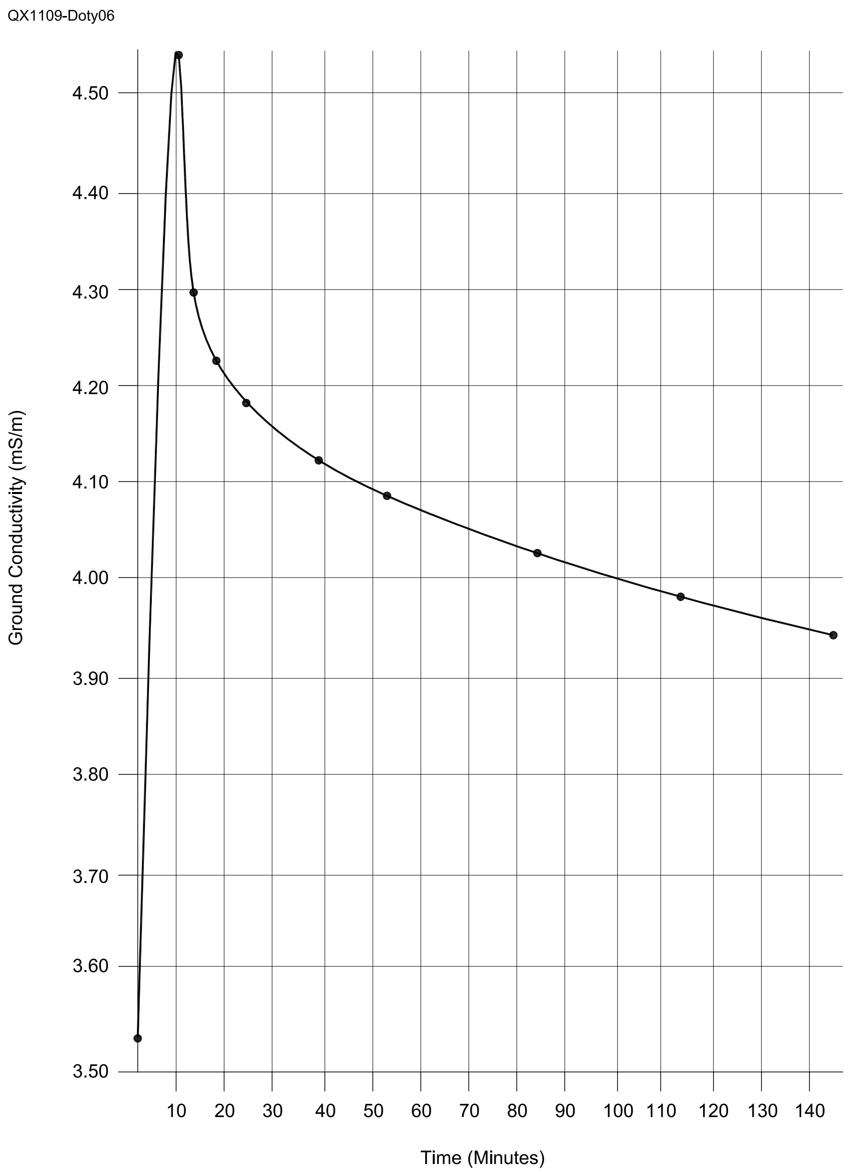

Figure 6 — This graph shows how the ground conductivity changed during the first 2½ hours after I soaked the ground to saturation.

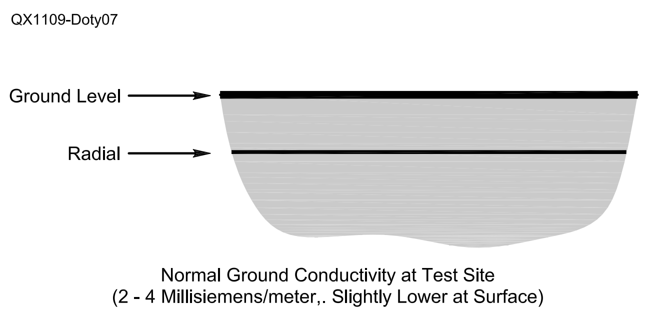

Figure 7 — Normal ground conductivity at my test site is 2 to 4 mS/m, with a slightly lower value at the surface, but fairly equal conductivity to a depth of about 8 inches.

for a short time after the rain ceases.

The hypotheses for this effect is:

When the rain falls, it is originally concentrated in the top few inches of the earth, which greatly increases the ground conductivity in this area.

The high conductivity in the area around the radials allows them to outperform elevated radials by making it easier for them to collect return currents both directly from the sky — through earth that now has higher conductivity — *and* from the area between the radials, again because the earth now has higher conductivity because of the heavy rain.

While this is happening, elevated radials merely maintain their usual level of performance, as they collect only those return currents that impact them directly from the sky, and none of those currents need to pass through soil.

After the rain has stopped the accumulation of water near ground level percolates into the earth, and the conductivity goes down in the top few inches — where the radials are located — to the point where elevated radials once again offer superior performance.

In order to learn more of the relationship between electrical performance and its moisture content a separate series of tests were performed.

In these tests the soil adjacent to antenna number 2 (buried radials) was soaked with water until the surface was saturated. Ground conductivity readings were obtained during the first eight minutes — while water was being applied — and at regular intervals thereafter. Figure 6 shows the result.

Figures 7, 8 and 9 illustrate what happens when the soil conductivity is greatly increased by heavy rain — as shown in Figure 6.

Figure 7 shows normal ground conductivity. It is nearly uniform from the surface, down four inches to the level of the radials, and then continuing down another four inches.

Figure 8 shows the ground conductivity immediately after a heavy rain. The darker the shade the higher the water content of the soil and the higher its ground conductivity. In this case the conductivity is highest at the surface and decreases as we go deeper into the earth.

Figure 9 shows the ground conductivity 2 hours after a heavy rain. Now the moisture has percolated into the soil and the surface has begun to dry. The higher ground conductivity is below the radial depth.

Practical Results

The basic aim of this test program was to develop new information on the electrical properties of the soil that surrounds antenna radials. From the data that resulted, several practical conclusions may be drawn. These are:

Unless there are practical or esthetic reasons for not doing so, it is more cost effective to locate radials under vertical antennas *on* the ground surface.

In areas of low ground conductivity, a dB or so of performance improvement may be obtained by elevating the radials, but the difference is so small that it will not be perceptible in practice.

In areas of high ground conductivity very slightly better performance can be obtained by burying radials. The improvement, however, will once again be imperceptible in practice.

As a matter of technical curiosity the FCC might want to reexamine its present requirements that there be 120 radials under Broadcast Band vertical antennas.[8]

The current FCC requirements are based on the 1937 study by Brown and others. Thus, they theoretically should apply only to areas where the ground conductivity is identical to that (not mentioned in the paper) at Brown's test site. As they are stated at present, the FCC requirements apply uniformly to all parts of the United States, although ground conductivity in different areas may vary by a factor of 60.

We now know that buried radials in high conductivity ground offer better performance. Thus, someone might consider that the current FCC requirements place an unnecessary physical and economic burden on stations built in areas of high ground conductivity — where, presumably, fewer radials are required for equal performance.

In reviewing the data presented in this article, we must remember that it represents tests conducted in a single area that has its own specific soil conditions and soil composition. Thus this information cannot be applied to other areas without additional testing.

As a matter of information, the FCC Ground Conductivity data referenced previously indicates that conductivity in the New Jersey area where Brown, Lewis and Epstine conducted their landmark study is identical to that at the Oregon site where my observations were made.

Some Notes About Atmospheric Noise

When I decided to use my existing antenna range to compare the performance of three antennas a problem immediately arose: When comparing two or more antennas the distance between each of them and the antenna providing the signal source *must* be exactly the same. As my three antenna sites were in a straight line, this was impossible. The answer was to use atmospheric noise as a signal source.

As noted in my article in the Mar/Apr 2011 issue of *QEX*, "atmospheric noise is the result of the very broadband electromagnetic impulses that are caused, primarily, by the 100 lightning flashes that occur every second somewhere in the world. These impulses (sometimes called "Sterics", or "Spherics") may propagate for thousands of miles from the lightning source without major attenuation in the earth-ionosphere waveguide.

Antennas operate by intercepting electromagnetic waves (including those created by lightning!) and converting them into electrical current for the receiver to amplify and detect. Thus there is a direct correlation between atmospheric noise levels and the signal strengths indicated by a communications receiver.

Atmospheric noise, when measured at 30 MHz on my ICOM 756PRO3, with both preamps operating, was entirely adequate to allow precise signal measurements. As these atmospheric signals are stable in the short term, they allow received signal strengths to be read with great accuracy. (Using W8WWV's *SMeter Lite* computer software program my S meter is a 9 inch wide bar-graph on a computer screen.)

There is almost no information in the Amateur Radio literature about atmospheric noise. Thus, both before and during the test program described in this article some additional tests were conducted, with interesting results.

How Constant Are Atmospheric Noise Levels?

To determine the difference between daytime and nighttime signal strength levels of atmospheric noise I recorded the data in Table 1.

What is the Polarization of Atmospheric Noise?

As I did not immediately find data on the polarization of atmospheric noise in the literature, I built a 10 meter dipole to explore the subject. This antennas is cut for 28.60 MHz — the same frequency as that of the three test antennas.

With the antenna center at about 8 feet off the ground, the ICOM 756PRO3 with one preamp operating, received atmospheric noise from this dipole as follows:

Horizontal signal strength –3.9 dB

Vertical signal strength +7.8 dB

These signal strengths were measured using the *SMeter Lite* software, and relate to the signal strength required to achieve an S 9 reading on the ICOM radio.

Thus, the vertically polarized component of atmospheric noise was 11.7 dB above the level of its horizontally polarized component.

From What Direction Does Atmospheric Noise Arrive at the Test Site?

This question was really academic, as the antennas being tested were omnidirectional. As a matter of curiosity, however, ten tests were made between August, 2010 and January, 2011.

In these tests the signal strength of atmospheric noise was measured, while my 3 element beam antenna at the top of a 75 foot tower was rotated 360°.

In five of the tests, the maximum signal strength of atmospheric noise was from the North. The other five tests showed maximum signal strength coming from the Northwest. In all of the tests there was zero signal coming from southern directions.

While these tests were being made, the world-wide, real time, occurrence of lightning activity (which caused the atmospheric noise) was monitored via the Internet. (Google "TOGA Lightning" and then select "TOGA Network Global Lightning Maps"). These maps clearly showed that the vast majority of global lightning discharges were in the tropical region, which is, of course, South of Oregon.

Why atmospheric noise arrives here from the North and Northwest, when its source is South presumably relates to the earth-ionosphere waveguide by which this radiation is transmitted. around the world.

To conclude my work with atmospheric noise I have recently conducted tests using a venerable General Radio signal generator, a modern transistorized signal generator and atmospheric noise as signal sources. The results were virtually identical, so I believe that the test data contained in this article is accurate.

Table 1
Variation of Atmospheric Noise Over Time of Day

Time (PDT)	*Relative Signal Strengh (dB)*
1645	–8.8
1700	–8.5
1745	–8.2
1805	–8.2
1835	–8.2
1855 (Dusk)	–8.2
1859 (Official sundown)	
1945 (Dark)	–8.1
2100	–8.1
2215	–8.2
0100	–7.9

Thanks

This test program ended up being, to a good degree, a communal project, with significant, useful and very much appreciated input from:

Greg Ordy, W8WWV. The test program could not have been conducted without his excellent software. Greg was also very helpful and tolerant when I had problems loading his program!

Bob Evans, W7RR, who contributed greatly with his years of knowledge from his AT&T and Amateur Radio experience.

Bill Conwell, K2PO, for his help in assuring that there are no inadvertent errors in this article.

Dick Frey, K4XU, The second generation of Freys (his father [SK] was John Frey, W3ESU) to provide much needed help with my antenna test programs!

Notes

[1]Brown, Lewis and Epstine, "Ground Systems as a Factor in Antenna Efficiency," *Proceedings of the IRE*, June 1937.

[2]FCC Rules and Regulations, Part 73.190 Subpart A, Figure R3.

[3]Arch Doty,W7ACD, "The Effects of Ground Conductivity on Antenna Radials", *QEX*, Mar/Apr, 2011, pp 1-4.

[4]Greg Ordy, W8WWV, "W8WWV's S Meter Lite Software," **www.seed-solutions.com/gregordy/Software/SMeterLite.htm**

[5]Jerry Sevick, W2FMI, "Measuring Soil Conductivity," *QST*, March 1981, pp 38-39.

[6]F. Wenner, "A Method of Measuring earth Resistivity," Bulletin of the Bureau of Standards, Vol. 12, pp 469-478, 1915-1916.

[7]Arch Doty, W7ACD, "Capacitive Loading of Vertical Antennas", **www.w7acd.com**

[8]FCC Rules and Regulations, Part 73.189, Subpart A, Paragraph (4).

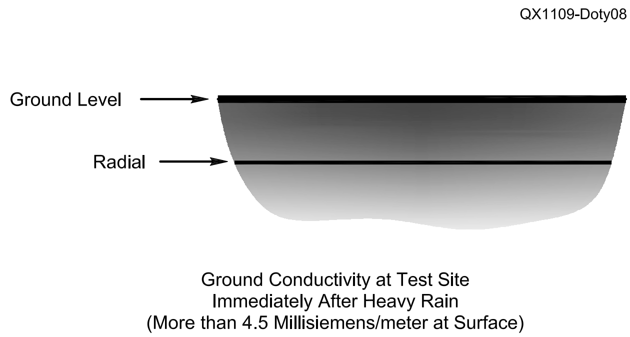

Figure 8 — After soaking the ground with water, the ground conductivity increased to more than 4.5 mS/m at the surface, but then gradually decreased to the original value at a depth of about 8 inches.

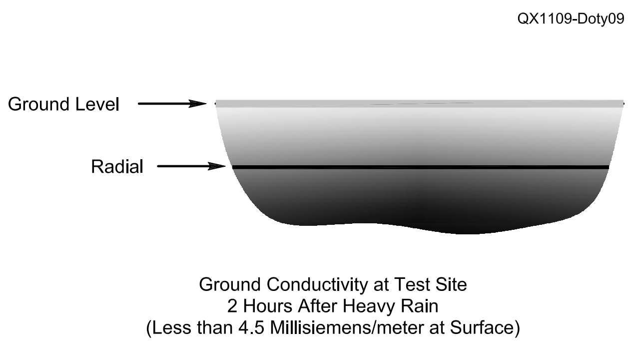

Figure 9 — Taking another set of measurements 2 hours after soaking the ground, I found that the conductivity at the surface had again decreased to the original value, but had increased to a higher value (more than 4.5 mS/m) at a depth of about 8 inches.

Fred Franke, WB2NFO

26 Dogwood Road, Kings Park, NY 11754; ffranke@suffolk.lib.ny.us

Playing With the Lambda Diode

This simple circuit provides many opportunities to experiment with applications of a negative resistance response.

From time to time articles appear in electronics publications describing the lambda diode, an interesting device that offers an alternate method of implementing various electronic functions. It is a two terminal component that exhibits a "negative resistance" between its terminals for a range of voltage applied across its anode and cathode. In other words, the current that flows through the diode decreases as the voltage across the diode increases. Its negative resistance characteristics are usually compared to those of tunnel diodes, which were somewhat popular years back, but are now rather scarce. Unlike the tunnel diode, the lambda diode is not manufactured as a discrete component, but is implemented by interconnecting two transistors.

In its most elegant form, the lambda diode consists of an N-channel JFET and a P-channel JFET cross connected as shown in Figure 1A. A typical plot of the current/voltage relationship of the lambda diode is shown in Figure 2. The negative resistance characteristic is exhibited in the range between points 1 and 2 on the curve.

The lambda diode has a number of possible applications, including amplifiers, mixers, bi-stable switches, and logic functions, but is most commonly used to implement oscillators. A parallel L/C tank circuit placed between the cathode of the diode and ground (or the anode of the diode and V_{CC}) will oscillate at the resonant frequency of the tuned circuit. The only limitation is that the Q of the tuned circuit must be high enough to ensure that its losses don't overcome the negative resistance of the lambda diode. Almost any typical L/C circuit will have sufficient Q to sustain robust oscillation. As a matter of fact if a dip meter is constructed around a lambda diode, it is often necessary to shunt the instrument's tuned circuit with a resistor to reduce its Q, so that the energy being drawn from the tuned circuit when

The author's test bed used to experiment with a variety of lambda diode applications.

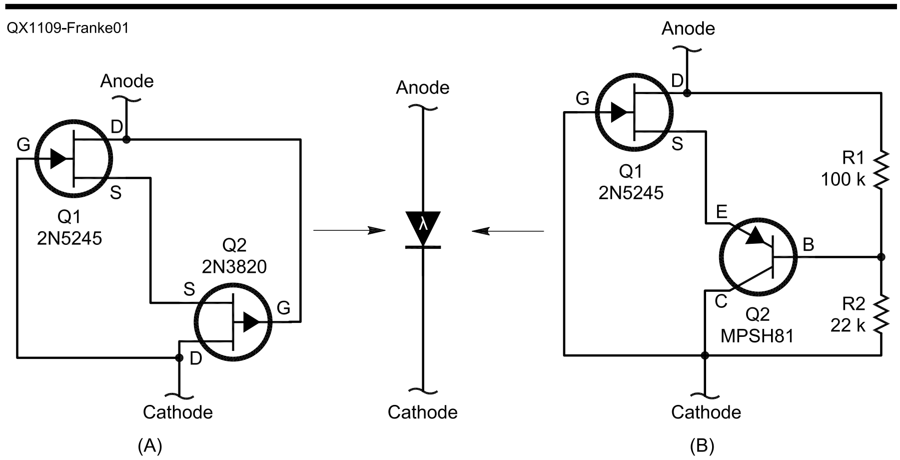

Figure 1 — A classic lambda diode using an N-channel and a P-channel JFET is shown in Part A. Part B shows a modified lambda diode, using an N-channel JFET and a bipolar transistor.

coupled to an external coil will produce a significant dip in the strength of the meter's oscillations. Additionally, the voltage developed across a high Q L/C circuit can be surprisingly large.

Neglecting stray capacitance and inductance, as well as the frequency limitations on the FETs used to implement the lambda diode, the device is frequency independent, and is therefore inherently a wide band device. It will sustain oscillations from audio to VHF/UHF, the upper limit being a function of the circuit layout and the FETs selected. All oscillators require positive feedback to sustain oscillation. The lambda diode provides this regenerative feedback between its two terminals rather than externally as with most conventional circuits. This results in a variety of applications implemented with very simple circuitry. For example, an attractive feature is that for most oscillator applications, the tuned circuit requires no tapped coils or split stator capacitors.

The classic lambda diode, as shown in Figure 1A, employs both an N-channel and a P-channel JFET. While fast N-channel JFETs are readily available, fast P-channel devices are less common. Even JFETs not characterized for high frequency applications, however, tend to work well into the VHF region. Another way to overcome the lack of fast P-channel JFETs is to modify the lambda diode to use a PNP bipolar transistor instead of the P-channel JFET. This configuration is shown in Figure 1B. Its characteristics are very similar to the classic two FET configuration. A lambda diode that I constructed using two low cost transistors, a 2N5245 N-channel JFET and an MPSH81 PNP bipolar transistor produced oscillations to over 200 MHZ.

Several papers on the Internet provide additional insight into lambda diodes and include some practical applications that would be of interest to hams.[1, 2, 3] I found circuits for dip meters, signal generators, a regenerative receiver, and audio oscillators. Three such interesting websites are listed at the end of this article.

The purpose of this article is to explore variations of the lambda diode that overcome some of the limitations of the traditional implementation. The electrical characteristics of the lambda diodes configured as shown in Figure 1 are totally defined by the

[1]Notes appear on page 19.

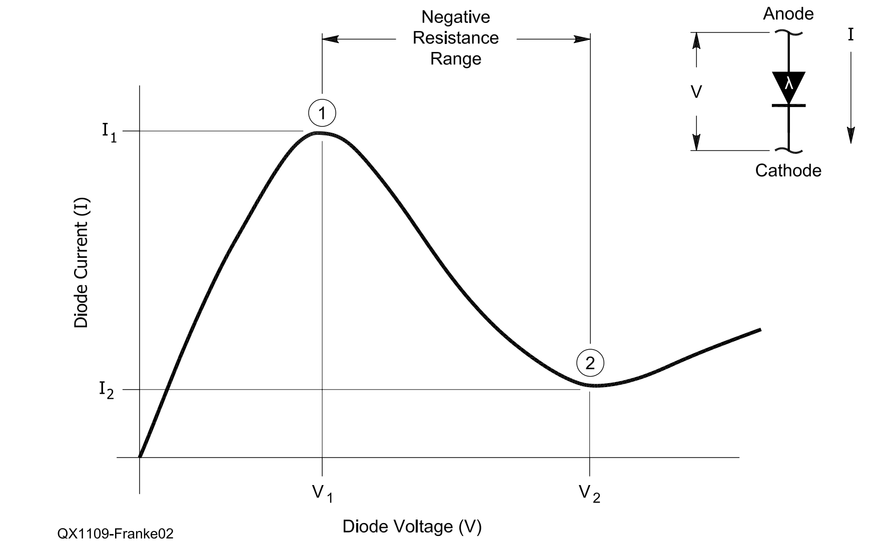

Figure 2 — This graph illustrates a typical lambda diode characteristic voltage/current curve.

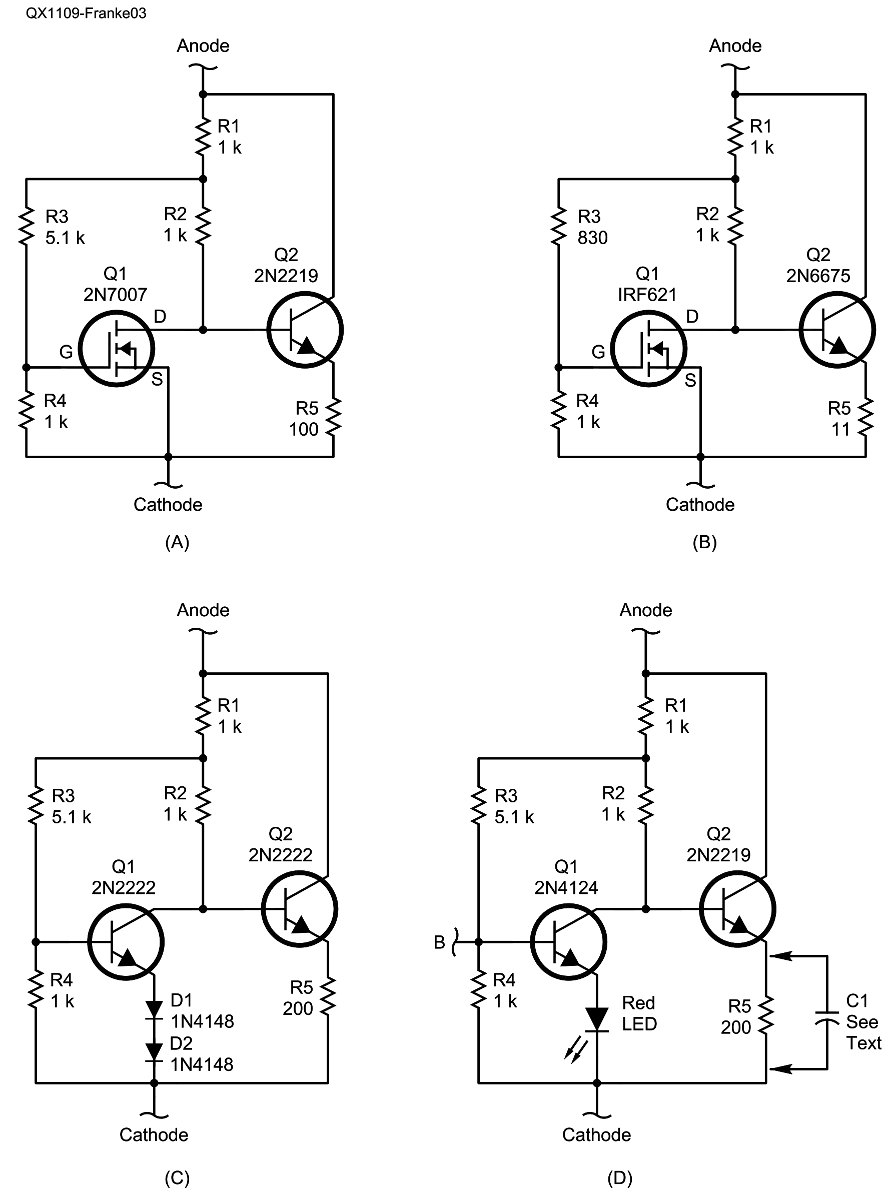

Figure 3 — Various programmable lambda diodes are illustrated. Part A shows the basic circuit. Part B is a high-power version. Part C shows a variation built from a pair of 2N2222 bipolar transistors. Part D is the bipolar transistor variation used to build the various applications described in the article.

two transistors selected, and are usually limited to operating currents of a couple of milliamperes and a peak voltage of about 10 V. I wanted to come up with a circuit that retained the general shape of Figure 2, but which could be setup for a wide range of currents and voltages, so that higher amounts of power could be developed if desired. A second goal was to achieve a circuit that would only require commonly available transistors. The configurations that resulted have undoubtedly been developed by others, but I was not able to find any published evidence of them to credit.

Programmable Lambda Diode

The initial implementation of a "programmable" lambda diode is shown in Figure 3A. Its operating characteristics are determined more by the values of the resistors than by the transistors themselves. It employs an N-channel MOSFET and an NPN bipolar transistor. Unlike the conventional lambda diode, in which the diode current flows equally through both transistors, in this configuration the bipolar transistor handles the bulk of the current, so only the bipolar transistor needs to have power handling capability. Figure 3A is a low power version while Figure 3B operates at higher power levels. The second two configurations implemented, shown in Figures 3C and 3D, replace the MOSFET with an NPN bipolar transistor. All four of the circuit configurations shown in Figure 3 produced characteristic curves similar to that of the traditional lambda diode. Table 1 lists the voltage and current levels measured for the resistance values provided in Figure 3.

The various applications described in the following paragraphs are based upon the lambda diode configuration of Figure 3D, since it can be implemented with virtually any of the most common and least expensive transistors that are likely to be found in the shack. Transistors used in the examples shown are devices that were readily available and do not represent transistors that might be more appropriate for a particular application. The circuit will realize negative resistance, however, with almost any pair of transistors that happen to be on hand. Of course the circuits shown in Figure 3C and 3D can be implemented with PNP devices if the direction of the diodes is reversed and the polarity of the power supply voltage is swapped. Note that the two forward biased diodes D1 and D2 in Figure 3C were replaced with a single red LED in Figure 3D. The red LED provides about the same bias voltage as the two silicon diodes, and as a bonus gives a rough visual indication of the current levels in the diode. If the base resistor, R5, is partially or fully bypassed with a capacitor (C1), the

Table 1
Characteristic Curve Parameters

Circuit Configuration	*V1 (V)*	*I1 (mA)*	*V2 (V)*	*I2 (mA)*
Figure 1A	1.8	1.7	5.9	0.05
Figure 1B	2.0	1.0	8.1	0.06
Figure 3A	15.0	89.	29.0	15.
Figure 3B	11.5	350.	22.0	60.
Figure 3C	15.0	50.	31.0	20.
Figure 3D	16.0	55.	32.0	20.

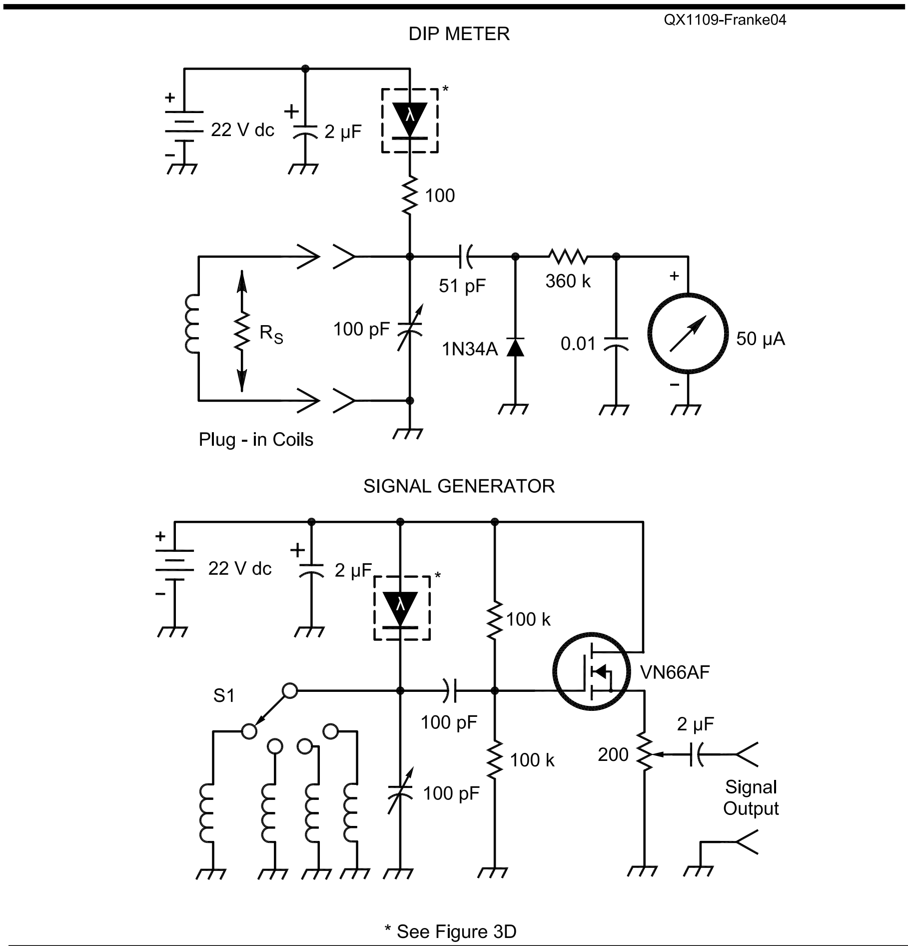

Figure 4 — A basic lambda diode dip meter circuit is shown in Part A, and a signal generator circuit is illustrated in Part B.

degenerative effect of R5 is reduced. With no capacitor, the diode produced oscillations up to about 20 MHz; with a 0.01 µF capacitor installed oscillations over 150 MHz were realized.

Programming the parameters of the lambda diode is accomplished by selecting the various values of the five resistors. Although there is some interaction among all five resistors, essentially the peak operating voltage (V1) is determined by the ratio of R3/R4, the current levels by R5, and the shape of the characteristic curve (Figure 2) by the ratio of R1/R2. If the ratio of R1/R2 approaches zero (R3 connected to the anode) the curve resembles the snap action of a thyristor device. If the ratio is large (R3 connected to the base of Q2) there is no negative resistance range. By letting R1 equal R2, the curve closely resembles the characteristics of the traditional lambda diode.

Applications

As mentioned earlier, a simple parallel tuned circuit placed in series with the lambda diode will oscillate at the resonant frequency of the circuit. Therefore, a very simple and wide range signal generator or dip meter can be implemented as shown in Figure 4. To make the signal generator practical, a source follower isolating stage and an output voltage amplitude adjustment potentiometer are included. If used as a dip meter, a simple detection stage must be added and, as noted previously, some of the coils may require a resistor shunted across them in order to get a good dip on the meter.

Crystal controlled oscillators are also easily implemented. Figure 5 shows one possible configuration for such an oscillator. Values listed are ones that worked well in my breadboard for crystals in the 3 to 4 MHz region. The circuit produced no oscillations with the crystal removed, and always started up on the fundamental frequency of the crystal when it was reinserted. The resonant frequency of the inductor and capacitor that seemed to work the best was somewhat above the crystal resonant frequency. The values shown allowed oscillation with crystals that spanned about one megahertz.

An unusual feature of the lambda diode is that if two L/C tank circuits are placed in series with each other, the configuration will oscillate on both frequencies. Figure 6 shows the schematic of a device that modulated the radio frequency controlled by L1/C1 at an audio frequency rate controlled by L2/C2. The shape of the modulated signal was not the typical amplitude modulation envelope, but consisted of approximately a half cycle of the audio sine wave followed by a 50% duration burst at the RF frequency.

The dc power source used during the evaluation of the various configurations and applications was a simple hefty variable dc power supply terminated at the breadboards with an electrolytic capacitor of several microfarads shunted with a 0.01 μF disk ceramic capacitor to simulate an "ideal voltage source." When experimenting with various external circuits, remember that regardless of where the power supply is placed in the circuit, there has to be a dc path through the lambda diode that biases the diode in its negative resistance range. A good starting point is to bias the diode in the middle of its negative resistance range. I found that 22 V was a good nominal voltage to start from if the resistor values shown in Figure 3D are used.

Most of the experiments that I conducted on the lambda diode were run in the 2 MHz to 10 MHz region, since circuit layout is not particularly critical at those frequencies, inductors are easily wound and the oscilloscope and other test equipment that was available performed well in that frequency range.

The lambda diode produces signal waveforms that range from clean sine waves to highly distorted waveforms that are usually associated with relaxation and blocking oscillators. Inductors employing iron cores seemed to be the most likely to produce nonsinusoidal signals. Wave shapes depend on a number of factors, but probably the single most significant factor causing the distorted sine waves is excessive drive to the L/C tank circuit. The waveform can be influenced by varying the operating point on the negative resistance range of the lambda diode by changing the operating voltage. Other methods include placing a resistor in series with or in parallel with the L/C tank circuit, deleting or reducing the value of C1 if it is being used, or by experimenting with different values for the programming resistors R1 through R5.

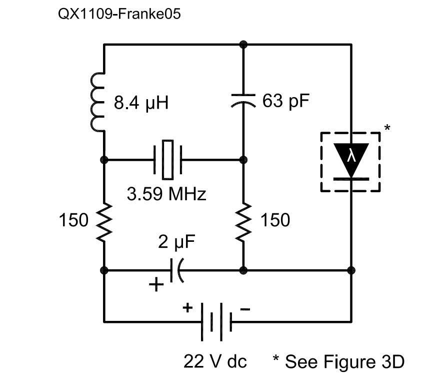

Figure 5 — This circuit is a simple crystal oscillator built using a lambda diode. The circuit will oscillate at the crystal frequency over a wide range of crystal frequencies.

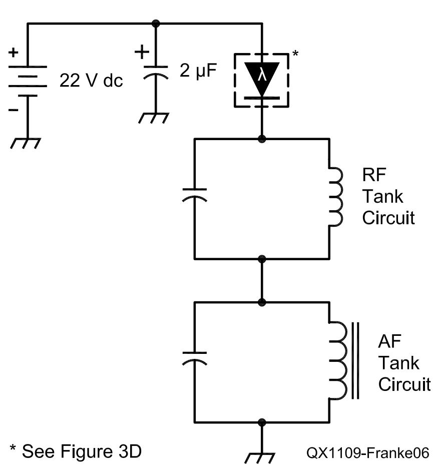

Figure 6 — This dual RF and AF oscillator will oscillate at two frequencies, with the RF signal chopped on and off at the audio rate.

The Lambda Triode

Another interesting feature of the circuits shown in Figures 3C and 3D is that if the cathode of the lambda diode is kept at ground potential, the base of Q1 is also at ac ground. This makes the base of Q1 a good point at which to inject an external signal in order to influence the circuitry being driven by the lambda diode. One application that worked very well, shown in Figure 7, was to couple the output of a crystal oscillator via a small capacitor into the base of Q1 (terminal B on Figure 3D). This caused the simple lambda diode oscillator circuit shown in Figure 4 to lock onto the crystal frequency over a fairly wide range of tank values. If the tank circuit was tuned to approximately twice the crystal frequency, a very stable frequency doubler was implemented. It was also possible to divide the crystal frequency in half by using a tank circuit tuned to approximately 50% of the crystal frequency. The frequency divider was significantly less tolerant of tank tuning than were the straight through and multiplier configurations. Other uses for this external input that suggest themselves might be amplitude or frequency modulation schemes, but I have not yet experimented with any additional applications for the lambda triode.

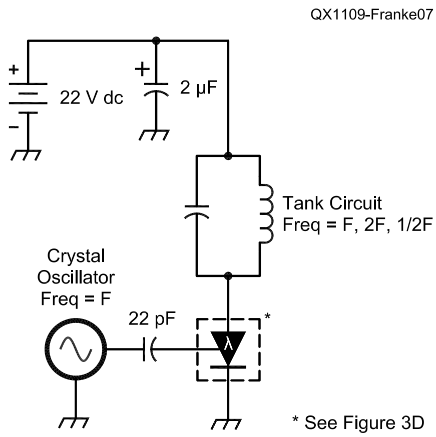

Figure 7 — With a crystal oscillator coupled to the base of Q1, a "lambda triode" circuit forms an effective frequency doubler or divide by 2 oscillator.

Test Bed

Although this is not a construction article, I did build up an enhanced breadboard intended to demonstrate some of the characteristics exhibited by circuits based upon the programmable lambda diode. The schematic of the test bed unit shown in the photographs is provided in Figure 8. Built on a wooden base using scraps of perfboard, the instrument uses the programmable lambda diode configuration detailed in Figure 3D to develop three simple instruments that might be useful around the shack. A six position rotary switch is used to select the desired function. In positions 1 through 4 the instrument functions as a Signal Generator in one of four selected frequency ranges. In position 5 the unit functions as an RF Code Practice Oscillator and in position 6 as a Dip Meter.

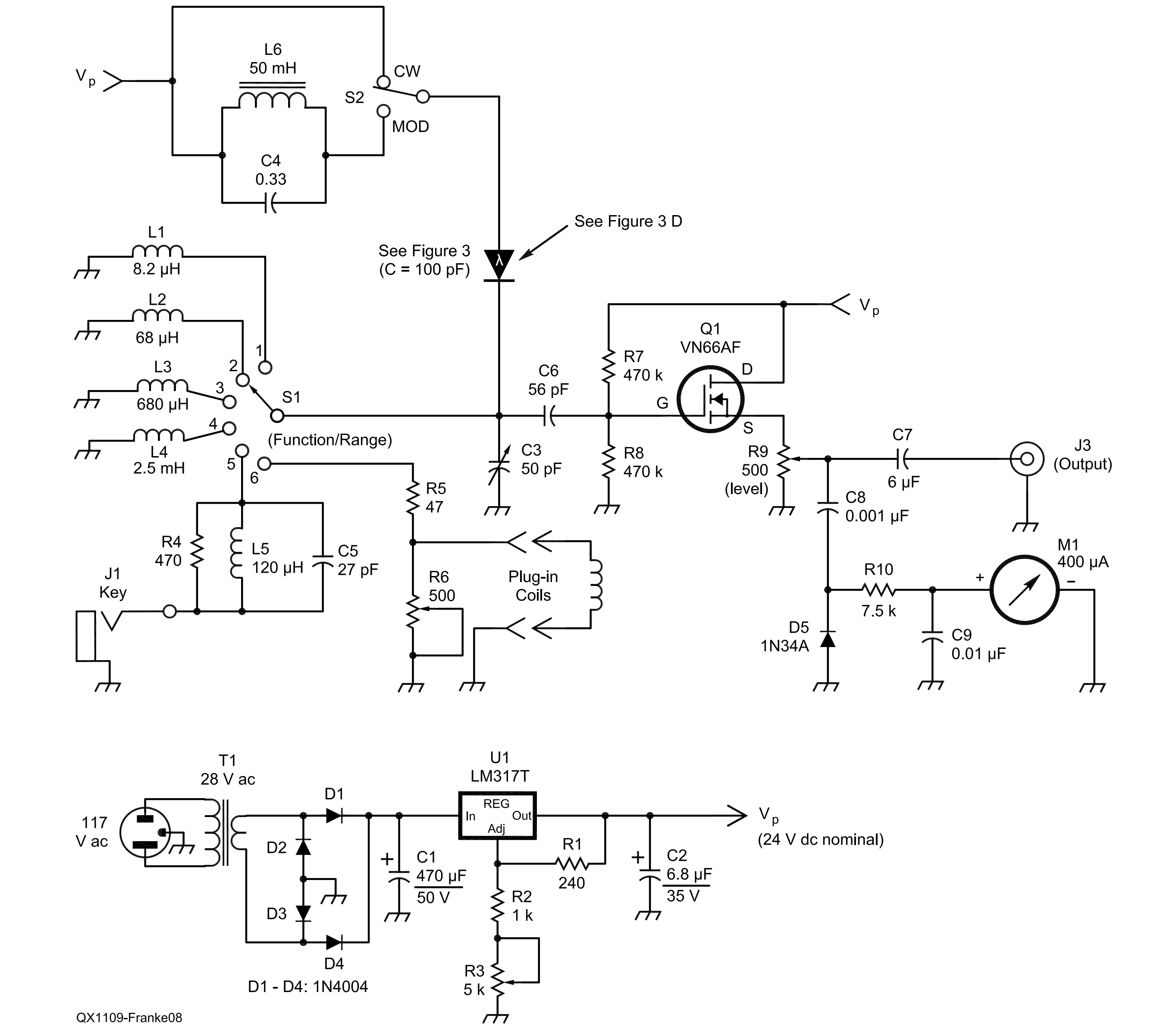

Figure 8 — The complete schematic diagram of the author's multi-function lambda diode test circuit. The first four FUNCTION/RANGE switch positions provide various signal generator frequencies, position 5 is an RF code practice oscillator and position 6 is a dip meter that uses various plug-in coils to establish the test frequency.

A built-in power supply featuring an adjustable output voltage allows observation of the lambda diode characteristics over various portions of its operating range.

The Signal Generator is a simple implementation of a lambda diode L/C oscillator. One of four inductors (L1 through L4) is selected by the FUNCTION/RANGE switch (S1) and the frequency is varied with a panel mounted variable capacitor (C3). The 50 pF variable capacitor used on my unit gave relatively narrow tuning ranges. Therefore I would recommend using a larger variable capacitor, perhaps 365 pF, if continuous frequency coverage is desired. The inductor for the lowest frequency range is a 2.5 mH RF choke and the other three inductors are air wound devices that happened to be on hand.

Using the values indicated on the schematic, the frequency range covered is approximately 250 kHz to 7.5 MHz (non-continuous). Adding a source follower stage isolates the output signal from the oscillator. It provides a relatively low output impedance and allows the signal amplitude to be varied using the LEVEL control (R9). A CW/MOD switch (S2) connects an L/C tank circuit (L6, C4), which is resonant at an audio frequency, in series with the anode of the lambda diode. This causes the RF to be modulated (perhaps more accurately described as interrupted) at an audio rate. With the values shown the audio rate is about 1 kHz.

The RF Code Oscillator, selected by placing the FUNCTION/RANGE switch in position 5, employs an L/C circuit (L5, C5) tuned to a spot in the AM broadcast band. The tuned circuit is placed in series with a jack (J1) to accommodate a telegraph key. The unit is placed near any AM radio, and the tuning capacitor (C3) is adjusted to find a dead spot on the band. Since most AM radios don't have a BFO, the CW/MOD switch would normally be placed in the MOD position when using this function. Resistor (R4) is placed across the L/C circuit to improve the waveform.

The Dip Meter is selected by placing

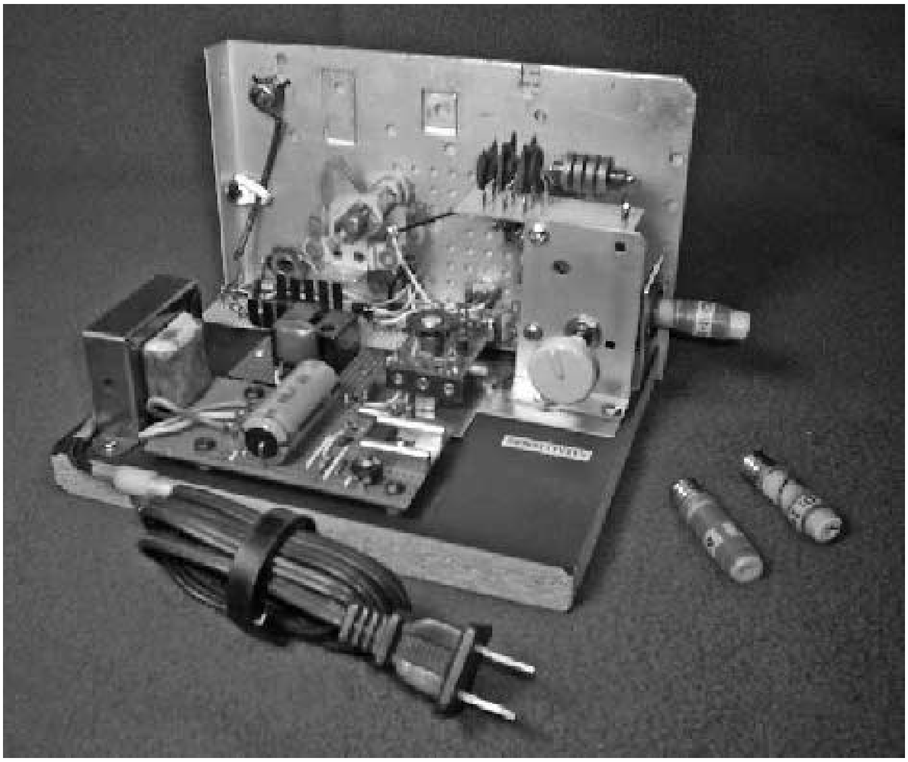

Figure 9 — This photo shows the circuitry of the author's lambda diode test bed.

the FUNCTION/RANGE switch in position 6. In this position, the inductors employed by the Dip Meter oscillator are plug-in coils wound to cover frequencies of interest. These coils are positioned to extend out from the unit to allow easy coupling to external circuits. One of the nice things about lambda diode oscillators is the fact that only two terminals are required for the tank circuits. Therefore it was possible to implement a set of plug-in (screw-in) coils using plastic rods inserted into the bases of candelabra lamps. A set of old Christmas lights provided the socket and plenty of bases for the coils.

The metering circuit takes advantage of the source follower that was already in place for the Signal Generator. It ties into the wiper of the LEVEL potentiometer, allowing the LEVEL control to set the meter to any desired position on the meter scale. Because the signal at the wiper of the LEVEL potentiometer is a low impedance voltage, it is not necessary to use a sensitive meter as the dip indicator. In my case a 400 µA subminiature meter was used. Just select the value of R10 as appropriate for the meter used. As mentioned earlier in the article, the lambda diode tends to produce robust oscillations. This masks the energy being drawn away by the tank circuit coupled to the Dip Meter coil. Therefore, a resistor (R5) and a potentiometer (R6) are included to reduce the level of drive to the plug-in coils. By properly adjusting the SENSITIVITY control (R6) a very deep dip can be obtained. The disadvantage, of course, is having this extra adjustment to contend with. In lieu of the potentiometer, a selected fixed resistor placed across each of the plug-in coils might do the job. The OUTPUT connector is a convenient place to attach a frequency meter to provide an accurate indication of the dip frequency.

Summary

Negative resistance devices are mentioned in many electronic texts but the topic is largely glossed over in most of these texts. It remains an interesting and somewhat undeveloped area of electronics. Hopefully this article will inspire some experimentation on negative resistance devices. The cost of gathering the parts for the basic diode should be less than a dollar if all the parts must be purchased, and will probably be zero for most hams since all of the components can typically be scrounged from almost any piece of defunct electronics. Even though the cost of damaging any of the devices used in this article is pennies, I found it very difficult to blow anything up since the lambda diode tends to be self protecting.

Perhaps the programmable lambda diode circuit presented in this article can be improved upon or tailored for a specific application. Maybe other versions of negative resistance diodes could be developed. The relative simplicity of circuitry needed to try out various ideas encourages experimentation. A low power transmitter based on a couple of stages of lambda diodes or triodes would seem to be an interesting little project to try.

Notes

[1]Larry Coyle, K1QW, Negative Resistance and the Lambda diode, **http://lcbsystems.com/LambdaDiode.html**

[2]Lloyd Butler, VK5BR, "A Dip Meter Using the Lambda Negative Resistance Circuit," **http://users.tpg.com.au/users/ldbutler/NegResDipMeter.htm**

[3]Ramon Vargas-Patron, "Oscillations and Regenerative Amplification using Negative Resistance," **www.zen22142.zen.co.uk/Theory/neg_resistance/negres.htm**

Fred Franke, WB2NFO, received his first Amateur Radio license (Technician) in 1970 and upgraded to Advanced in 1978. He earned a Bachelor of Electrical Engineering degree from the City College of New York (CCNY). Now retired, Fred spent most of his career as an engineer designing cockpit instruments for numerous military and commercial aircraft. Currently, he consults on redesigns of out-of-production electronics in older aircraft. QEX

Jukka Vermasvuori, OH2GF
Viputie 3, FI-01640 Vantaa, Finland; **jukka.vermasvuori@luukku.com**

Measuring Coils In Tuned Circuits For Short Wave Frequencies

Are coils problematic components in your designs? Tuned circuits are still valuable in the IC era!

Constructing your own short wave amateur equipment requires basic measurement capabilities. Voltages and currents: dc and ac, resistance and capacitance. All these can be measured with reasonable accuracy using a low-cost hand-held multimeter. Measuring frequency is more rewarding. Today's digital technology has created simple frequency counters, which are available either in kit form or ready made. Some investment is needed, however.

Measuring inductance is more complicated. To make real coils, in addition to the inductance you must also have knowledge of the coil losses, indicated with Q_0 values. You must know the Q_0 value *on the very frequency on which you are intending to use the coil*. Making air wound solenoid coils is well covered in the literature. *The ARRL Handbook* gives rules to construct coils with the desired inductance.[1] Q_0 values are not directly calculable, however. Modern equipment design requires small size, and therefore most of the coils today are of toroidal form and they use various ferrite or iron powder cores to increase the inductance. The real problem with this type of construction is the great variation of losses depending of the core material versus frequency used. To construct coils with predictable values, you must have knowledge of the coil Q_0 on the frequency used. Some kind of Q-meter is needed. Coil bridges using some fixed frequencies in the low short wave range are not useful.

The following shows a simple solution to measure coil inductance and Q_0 values on the desired short wave frequency.

L and Q Meter

The basic idea is to use the coil to be measured as part of parallel tuned circuit in an LC oscillator. For practical reasons one end of the coil should be grounded, and be tuned to the desired frequency with a parallel calibrated variable capacitor. The amount of feedback around the oscillator should be continuously adjustable and be calibrated to make the Q_0 value calculable. High Q_0 coils need less feedback to start oscillations.

An external counter is used to indicate that oscillation has started, as well as the frequency. A basic four function calculator will help us find $L_{(\mu H)}$ and Q_0.

Parallel Tuned Circuits Basics

Figure1A is lossless parallel tuned circuit. Part B represesnts a practical case, in which most of the losses are in the coil. Resistor R is the simulated coil loss. In part C, the coil loss, R, has been transferred to a parallel loss resistor, R_0. At resonance, the inductive and capacitive reactance values are of the same magnitude and opposite sign, to cancel each other. The remaining R_0 indicates the losses in the circuit. In practice it includes all the losses in the tuned circuit, including possible negligible losses in the capacitor.

R_0 is the resistance of the tuned circuit at resonance and is used for the calculation of stage gain in an active device amplifier. Higher R_0 means higher gain. In an amplifier circuit Q_0, R_0, is never reached due to load-

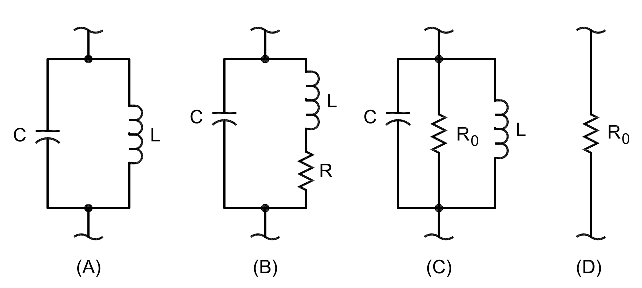

Figure 1 — Part A represents a perfect lossless parallel tuned circuit. In Part B, we have the addition of some inductor losses, represented by *R*. Part C shows the result of changing the series loss resistance, *R*, to a parallel resistor, R_0. In Part D we see the effects of resonance on our circuit. The inductive and capacitive reactances are equal and opposite, so the only remaining part of the impedance is the parallel resistance, R_0.

[1]Notes appear on page 24.

ing of the amplifier output resistance and the next stage input resistance. Taking these into consideration, loaded Q_L is calculated.

The selectivity and bandwidth of a tuned amplifier is directly related to the loaded Q_L value. The separation of –3 dB points on the selectivity curve are found by dividing the resonant frequency by the loaded Q_L, as given in Equation 3.

At resonance:

$$L(\mu\mathrm{H}) = \left(\frac{159}{f(\mathrm{MHz})}\right)^2 \times \left(\frac{1}{C_t(\mathrm{pF})}\right) \quad \text{[Eq 1]}$$

By knowing C and f, L can be calculated. By knowing L and f, C can be calculated. C_t is the total capacitance in parallel with the coil.

$$R_0 = Q_0 \omega L = \frac{Q_0}{\omega C_t} \quad \text{[Eq 2]}$$

where Q_0 is the coil Q without external loading.

$$\Delta f_{-3\text{ dB}} = \frac{f_0}{Q_L} \quad \text{[Eq 3]}$$

Making the Oscillator

Some portion of the output signal must be fed back to the input. In the oscillator shown in Figure 2, the output sample is taken with a small capacitor, C_{s1} to a 50 Ω resistor, working as the input resistance of the amplifier, A. The amplified signal is across a second 50 Ω resistor and is returned to the tuned circuit via an additional small C_{s2}. Both small capacitors are chosen to be of the same value, and are in practice half of a tuned variable capacitor.

Figure 3 shows the transformation of series R_s and C_s to their parallel form, R_p and C_p.

$$R_p = R_s + X_s^2 / R_s \quad \text{[Eq 4]}$$

$$X_p = X_s + R_s^2 / X_s \quad \text{[Eq 5]}$$

In our case, the small C_s means high X_s, compared to R_s = 50 Ω and allows us to simplify Equations 4 and 5:

$$R_p = X_s^2 / R_s \quad \text{[Eq 6]}$$

$$X_p = X_s \quad \text{[Eq 7]}$$

Adding a tuned circuit between the source and load causes insertion power loss, A. Additionally, matching the generator to the load adds some loss. To make an oscillator, we will need an amplifier with gain A_t to overcome losses. The total gain around the oscillator is one. Matching with high X_s (low C), the current in series, C_s + 50 Ω is almost capacitive, with a 90° phase shift, so two of them make a phase shift of close to 180°. This is canceled with the 180° phase shift of amplifier A, making the net phase shift 0°. Higher gain in amplifier A allows lighter loading of the LC circuit.

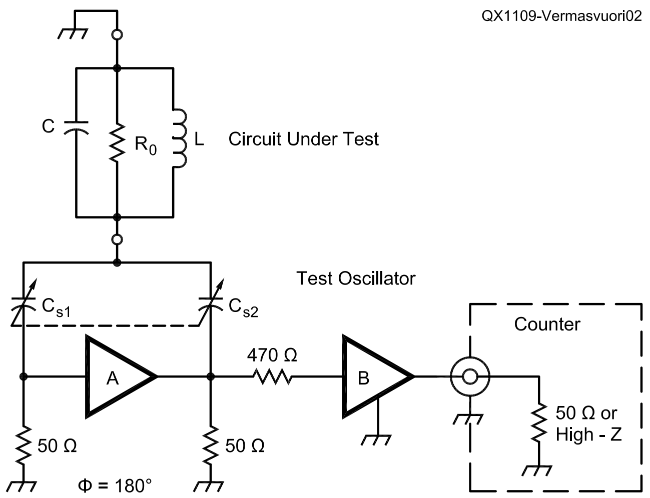

Figure 2 — This diagram illustrates the basic circuit used to measure inductance and Q_0.

TABLE 1

Q_L / Q_0	A	A (dB)	√A	1 / √A	1 / √A –1	A +6 (dB)	A_{tot} (dB)
0.7675	0.05406	–12.67	0.2324	4.30	3.30	–12.67 +–6	–18.67

Used amplifier gain is 18.7 dB, so , $1/\sqrt{A} - 1 = 3.30$, which is used in Equation A9.

Finally:

$$Q_0 = \frac{482\ C_t(\mathrm{pF})}{f(\mathrm{MHz}) \times C_s^2(\mathrm{pF})} \quad \text{[Eq 9]}$$

Two 50 Ω terminations are transformed in parallel to the tuned circuit. In the circuit presented here, the amplifier gain 18.75 dB has been used. Higher gain means smaller C_s in picofarads and makes a small 3 to 16 pF capacitor useful.

Making Measurements

Connect the coil to be measured between the coil terminals. Switch the internal variable C to be in parallel with the coil. Tune C so that it provides the desired parallel capacitor value C_t that you intend to use. $C_t = C + 2C_s + 10$ pF. If you are measuring a ready-made circuit with internal parallel capacitance, (such as an IF can), leave the switch open.

Apply 12 V to the circuit and connect the frequency counter to the output. Begin to increase the feedback capacitor C_s from minimum and observe the point where the oscillator starts to oscillate, giving a reading on the counter. Note the values of C, C_s and frequency. The total C_t in parallel to the coil is: $C + 2C_s + 10$ pF. (If you are measuring an IF-can, C is replaced with the internal C inside the can.) Now you know the total parallel capacitance and frequency of the oscillation, The inductance, L, can be easily calculated from Equation 1. The value of C_s is related to the coil Q_0, which can be calculated from Equation 8 or 9.

$$Q_0 = \frac{1592\ C_t(\mathrm{pF})}{\left(\frac{1}{\sqrt{A}} - 1\right) \times f(\mathrm{MHz}) \times C_s^2(\mathrm{pF})} \quad \text{[Eq 8]}$$

where:
$C_t = C + 2C_s \pm 10$ pF
C_t and C_s are in pF and f is in MHz.
The term $(1/\sqrt{A} - 1)$ is given in the Appendix, If a different loss/amplifier gain is used, see Table 1.

For example, if using an 18.75 dB amplifier:

$$Q_0 = \frac{482\ C_t(\mathrm{pF})}{f(\mathrm{MHz}) \times C_s^2(\mathrm{pF})} \quad \text{[Eq 9]}$$

If you are not directly interested to the numeric value of Q_0 you can easily compare the quality of different coil candidates *on the desired frequency* by watching the size of C_s needed. Less C_s means higher Q_0, keeping C constant. Higher C needs higher C_s to start oscillation.

Other Applications

You can even check the activity of a quartz crystal by connecting it to the coil terminals. Leave the C switch open. Starting from minimum C_s you look for oscillation with the parallel mode and you have the frequency depending on C_s. To find the operating frequency of a 32 pF crystal, you will need a C_s of 11 pF. (32 = 2 × 11 + 10).

You can also use this circuit as a simple RF generator with an external attenuator unit.

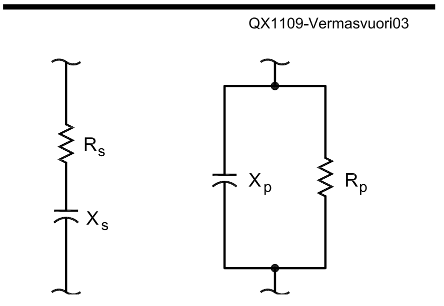

Figure 3 — Here we see the transformation of series to parallel circuit resistance and reactance.

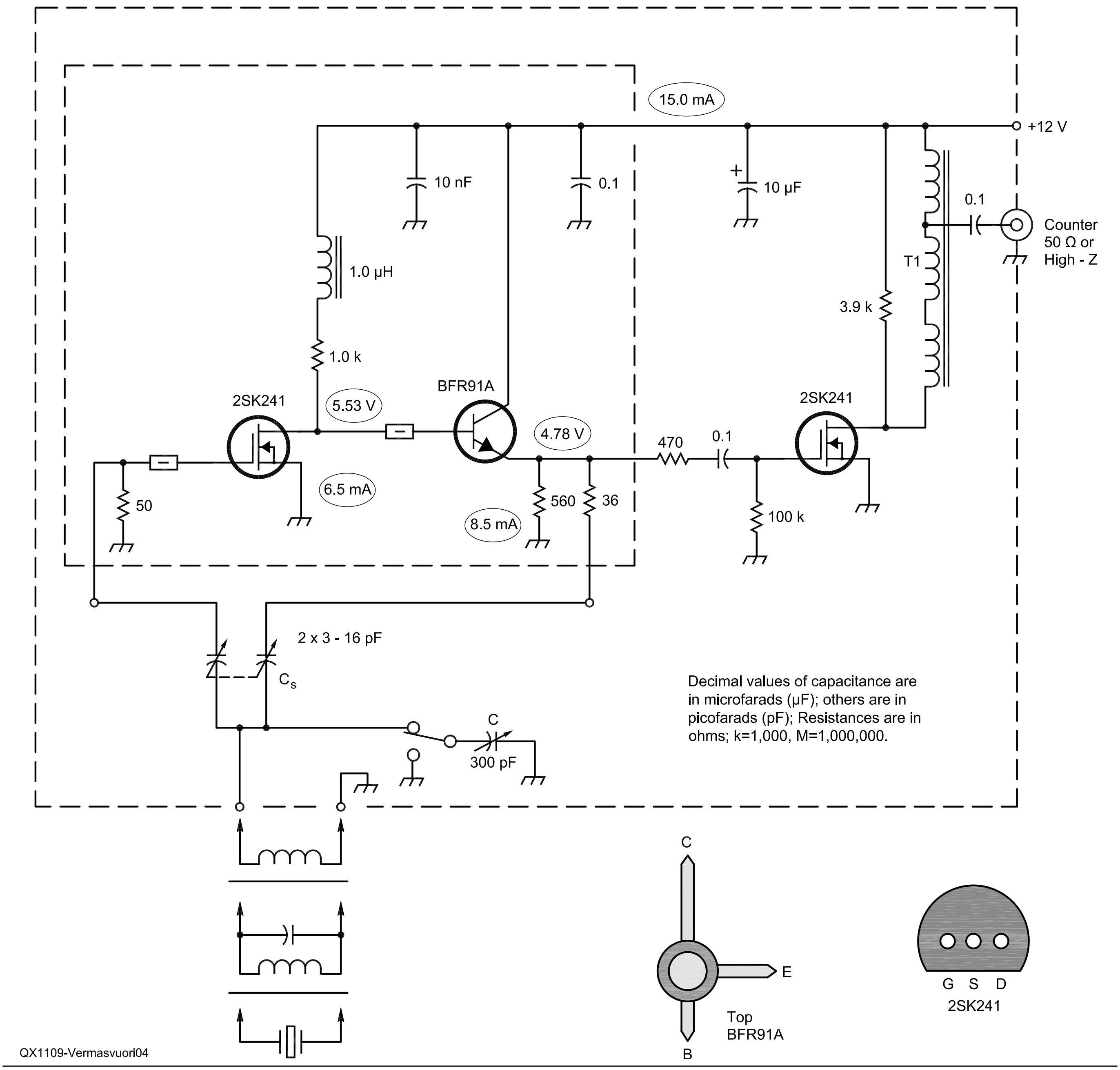

Figure 4 — This schematic shows the complete test circuit. The amplifier input resistor is a 49.9 Ω, 1% unit. For the output series resistor, the optimum value is 35.7 Ω, and the nearest standard value is 34.7 Ω, 1%.
T1 is a trifilar transformer: 13 turns, 3 strands of 0.2 mm copper wire twisted, on 9 mm toroid. The toroid is a Ferroxcube 4A11, μ_i = 850, pink, similar to an Amidon T-37-43.
DC values are in no oscillation condition. C_s is set at minimum.

An interesting test is to couple your antenna parallel to the 50 Ω amplifier input by an external cable and feed the counter output to your receiver. Start C_s from the minimum. Now you have a preselector with an adjustable regenerative high *Q* selective tuned circuit. Be careful because it can put a relatively high signal level into the receiver when oscillation starts!

Because Q_L is close to Q_0 (0.77) the coil is very sensitive to the surrounding effects. This circuit phenomenon is useful as a grid dip meter or metal detector circuit in the field.

Practical Equipment

Figure 4 shows the schematic diagram. Figure 5 shows the front panel of my completed test set. For outside connections, two banana terminals are used, one for the hot coil terminal and another for the coil ground connection. The internal calibrated 300 pF air variable capacitor, *C*, is behind a switch. When *C* is not in use it is grounded by the opposite terminal of the switch.

The feedback capacitors are two 3 to 16 pF air variable capacitors from an old FM receiver. It includes a gear, so the knob has a range of 1.5 turns, which is a great help to make a more accurate calibration in picofarads. The knob is *calibrated with the single half unit,* one of the 3 to 16 pF capacitors. As the body of this capacitor is hot with RF, it must be installed so it is isolated and the shaft and knob can be plastic to reduce the influence of hand capacitance. Actually, the capacitor body was screwed to an aluminum support, which is bolted directly to the hot banana terminal screw. See Figure 6.

The broadband amplifier, A, is a two stage amplifier, with a 2SK241 and a BFR91A transistor. The circuit uses ground plane construction, and short by-pass capacitors and resistors are soldered vertically to the small piece of copper clad circuit board material. Transistors are elevated the length of the by-passes from the ground. This print is located on the side of the C_s variable capacitor in a vertical position to minimize the length of amplifier input and output connections. The print is fixed by soldering spots to the front panel double sided copper clad circuit board material.

The 1 μH inductance at the 2SK241 drain is a peaking coil to flatten the frequency response towards the upper end.

The unloaded voltage gain is 18.75 dB. The –1 dB point is over 100 MHz. The output impedance should be 50 Ω. By computer simulation, the output resistance starts to increase after 20 MHz, being 51 Ω at 30 MHz and 54 Ω at 50 MHz. This checking can be done also with an oscilloscope by temporarily loading the C_{s2} connection with a dc isolated (0.1 μF) 50 Ω resistor. Feeding

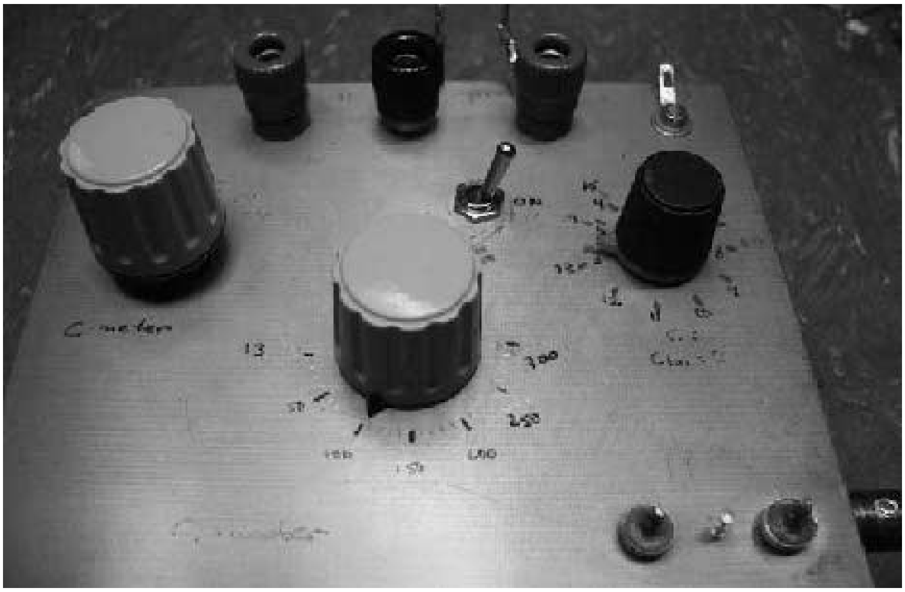

Figure 5 — Front view of the prototype equipment. It includes C-meter, gray knob and red banana terminal on the left that is not included in this presentation. The coil terminals are black and red on the right.

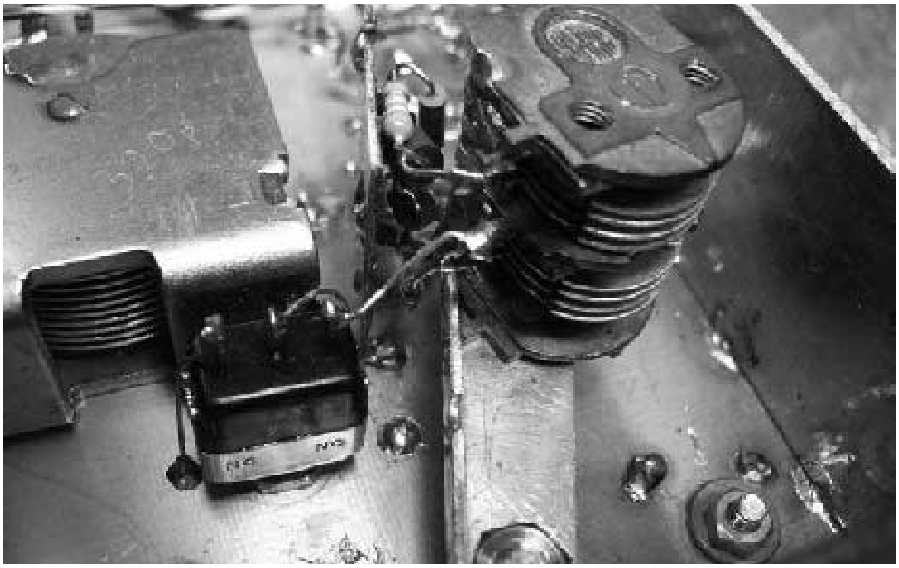

Figure 6 — Detail of the circuitry. The double variable capacitor, C_s, is on the aluminum support fixed under the hot coil terminal nut. The amplifier print is vertical behind the variable capacitor C_s.

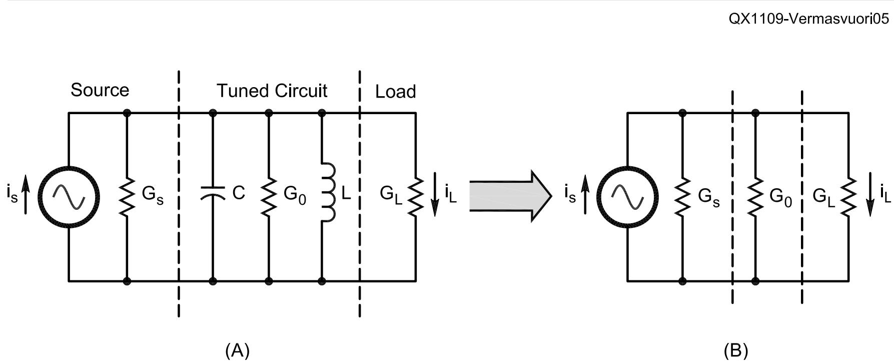

Figure 7 — The resistance values have been converted to conductances to simplify the calculations in the parallel circuit. The tuned circuit has been added between the source and load, and at resonance the inductive and capacitive reactances are equal and opposite in value, so they cancel out.

the generator to the amplifier input, with C_s set to minimum, the output RF voltage should drop to half with this external 50 Ω resistor.

This amplifier was stable with generator feed and 10:1 probe load. When installed in the real circuit with the C_s source and load, a very high frequency self oscillation occurred. To tame it down, a ferrite bead was used at the 2SK241 gate and at the BFR91A base lead.[2] The start of normal oscillation should be smooth and return back to off without hysteresis.

The buffer stage with the 2SK241 is not located on the original circuit board, but is constructed separately on the back side of the front panel using ground plane construction.

The reason to use the 2SK241 is that its transconductance with zero bias is 10 mA/V and feedback C = 0,035 pF. It is competing with dual gate MOS FET qualities but needs five fewer components to realize the proper bias conditions. To guarantee adequate drain-source voltage in the first stage, an FET with lower end of I_{DSS} selection GR, 6 to 14 mA is needed. It would be better to select a device with Y of 3 to 7 mA, but one was not available.

Notes

[1]H. Ward Silver, NØAX, Ed, *The ARRL Handbook for Radio Communications*, 2011 Ed, Chapter 2, "Electrical Fundamentals," pp 2.49-2.52. ISBN: 978-0-87259-095-3; ARRL Publication Order No. 0953, $49.95. ARRL publications are available from your local ARRL dealer or from the ARRL Bookstore. Telephone toll free in the US: 888-277-5289, or call 860-594-0355, fax 860-594-0303; **www.arrl.org/shop**; **pubsales@arrl.org**.

[2]M. Chessman, N. Sokal, "Prevent Emitter-Follower Oscillation," *Electronic Design*, 13, June 21, 1976 p 110-113.

[3]W.Th. Hetterscheid, "Transistor Bandpass Amplifiers," *Philips Technical Library*, p 283-288.

[4]Manasse, Ekiss, Gray, *Modern Transistor Electronics, Analysis and Design*, Prentice-Hall, Inc, USA, (Chap 5, Tuned Amplifiers) p 150

[5]Amidon, *Tech Data Book*, **www.amidoncorp.com/specs/1-18.PDF** .

[6]F. Langford-Smith, *Radio Designers Handbook*, London, Iliffe & Sons, Ltd, 1953, 4th Edition, p 467-470.

Appendix

Calculations for Q_0

For easier calculations, the resistances are replaced by conductances, where $G = 1/R$

Figure 7 presents the situation where a tuned circuit has been added between the source and load.[3, 4]

A_{tot} is the sum of all losses.

$$A_{tot} = A_{source/load} \times A \qquad \text{[Eq A1]}$$

The first term is loss between the source and load. When $R_s = R_L$, loss is 6 dB.

The second term is the insertion loss of adding the tuned circuit. (See Notes 3 and 4.)

$$A = \left(1 - \frac{Q_L}{Q_0}\right)^2 \qquad \text{[Eq A2]}$$

A is power loss, A(dB) = 10 log A , $A < 1$, so A is negative in dB

It can be shown, that:

$$\frac{Q_L}{Q_0} = \frac{G_0}{G_s + G_0 + G_L} \qquad \text{[Eq A3]}$$

and when $G_s = G_L = G$

fitting Equation A3 to A2:

$$A = \left(1 - \frac{G_0}{2G + G_0}\right)^2 \qquad \text{[Eq A4]}$$

from this, G_0

$$G_0 = 2G\left(\frac{1}{\sqrt{A}} - 1\right) \qquad \text{[Eq A5]}$$

and then converting back to resistance:

$$R_0 = \frac{R}{2\left(\frac{1}{\sqrt{A}} - 1\right)} \qquad \text{[Eq A6]}$$

$$\frac{R}{R_0} = 2\left(\frac{1}{\sqrt{A}} - 1\right) \qquad \text{[Eq A7]}$$

$R_0 = Q_0 / \omega C_t$ from Equation 2, and

$R = X_s^2 / 50$ from Equation 6.

Solving for Q_0:

$$Q_0 = \frac{C_t}{628\left(\frac{1}{\sqrt{A}} - 1\right) \times f \times C_s^2} \qquad \text{[Eq A8]}$$

Using capacitance in pF and frequency in MHz:

$$Q_0 = \frac{1592 \times C_t(\text{pF})}{\left(\frac{1}{\sqrt{A}} - 1\right) \times f(\text{MHz}) \times C_s^2(\text{pF})} \qquad \text{[Eq A9]}$$

Required Amplifier Gain

The total loss, A_{tot}, around the oscillator is the sum of:

1) Loss between the source and load resistors.

When $R_g = R_L$, the voltage at the output drops to half, meaning there is a 6 dB loss, independent of the value of C_s!

2) Tuned circuit insertion loss, A.

$$A_{tot} = -6\text{ dB} + A \qquad \text{[Eq A10]}$$

and in dB:

$$A_{tot}\,(\text{dB}) = -6 + 10 \log A \qquad \text{[Eq A11]}$$

Total loss is compensated by the amplifier gain, A_t, to have a net effect of 1, or 0 dB. The loss components are presented in Table 1.

Comparing Results

To verify the validity of Q_0 measurement, no standard coil with measured Q_0 was available. For iron powder toroids, Amidon has given some Q_0 curves for reference in their *Tech Data Book*, on pages 1-18.[5] I made one of those reference coils using a T50-6 core with 34 turns, using 0.4 mm copper wire, instead of no. 24 AWG, which has a diameter of 0.51 mm. I measured Q_0 = 232 around mid frequencies, and the *Tech Data Book* gives a reference Q_0 = 263. Toward the lower frequencies, however, the measured Q_0 was slightly smaller than the reference. Using the 0.4 mm wire instead of 0.51 mm wire decreases the Q value!

I inspected several sources for air wound coils to find a suitable reference. Most calculated Q_0 values were rather high and probably were not to be trusted. The best practical indication came from *Radio Designer's Handbook*.[6] According to rules given on pages 467 to 470, I wound a 9½ turn coil on a ⅝ inch form using 1.1 mm copper wire, and measured the Q_0 with a different C_t. Measured results were also about 15% on the low side at mid frequencies. It is a problem to calibrate and read low C_s values accurately, (0.1 pF), so some variation in the measured Q_0 result is to be expected. QEX

Maynard A. Wright, W6PAP

6930 Enright Dr, Citrus Heights, CA 95621; w6pap@arrl.net

Octave for Curve Fitting

Maynard presents another set of functions available in Octave. *This time he shows us the least squares curve fitting function.*

Antenna Problems

We are a bit late in setting up for Field Day and we have just erected our 40 meter CW antenna. We have cut it for 7.050 MHz using the familiar 468 / f (MHz) formula and we've strung 60 feet of 450 Ω window line between the center of the antenna and our operating position.[1] Before we connect the transceiver, we'll check our installation with an antenna analyzer. But what's this? The analyzer tells us that the antenna is resonant at about 7.23 MHz. What have we done wrong? We run to the 80 meter operating position to borrow their analyzer, but it simply confirms what ours already told us. Did we measure our 12 gauge wire incorrectly? Are ground effects (our height is 25 feet) shifting things more than we might expect? Should we tear down the antenna and try again?

Modeling the Antenna

Our antenna is actually just fine and we ought to go ahead and enjoy Field Day. What, though, is wrong with our analyzer measurement? Nothing except our interpretation of it. Now that Field Day is over and we're back at home, let's use the input impedance code we developed in *Octave for Transmission Lines* to look at our entire installation, consisting of the antenna and the transmission line.[2]

First, though, we need a good model of what we think the antenna ought to do. We will use the antenna modeling program *nec2c* that we've used previously in this series on *GNU Octave*.[3,4] We will assume that our Field Day antenna was a center-fed dipole 25 feet above ideal ground using 66.4 feet of no. 12 gauge wire. We would like to look at the performance of the antenna and transmission line at tightly spaced frequencies around our intended operating frequency over a range of, say, 2 MHz from 6 MHz to 8 MHz. We could use *nec2c* to generate numerous input impedances for a large number of frequencies but that would be very tedious. Instead we'll try something else.

We will begin by calculating the input impedance at 500 kHz intervals over our frequency range of interest. That involves five invocations of *nec2c*, or your favorite antenna analysis program, from 6 MHz to 8 MHz. The results are listed in Table 1.

We can plot these using some of the *Octave* code in Table 2, and the result is shown in Figure 1. The third plot specified in *plot* in Table 2 produces the horizontal line at an impedance of zero, added for clarity. The third argument, "-," to each plot specification draws a straight line, quantized as necessary, between the various points in each

Table 1
Input Impedance of 66.4 Foot Center-Fed Dipole

Frequency (MHz)	*Resistive Component (Ω)*	*Reactive Component (Ω)*
6.0	26.91	–254.8
6.5	38.10	–131.0
7.0	52.94	–10.78
7.5	72.47	108.6
8.0	98.06	229.2

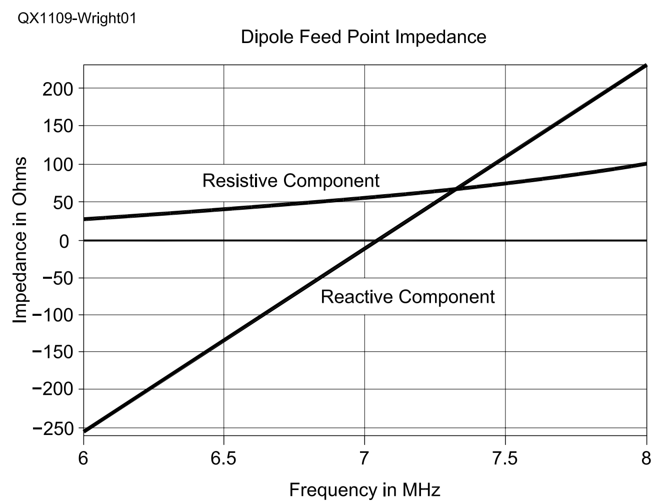

Figure 1 — Impedance of dipole with linear interpolation between points.

[1]Notes appear on page 29.

plot. The *Octave* code used in this article is available for download from the ARRL *QEX* files website.[5]

At this point, we have a couple of nice curves that look very much as we would expect a dipole to behave over a limited range of frequencies near resonance if we compare our plots of resistance and reactance with the corresponding section of Figure 2 on page 2-3 of Chapter 2 of *The ARRL Antenna Book*.[6, 7] We still don't have a way, though, to model our antenna mathematically at any frequencies in between the five 500 kHz spaced frequencies that we used to generate the sequences of straight lines that constitute the two curves.

If we can fit curves to the antenna impedance data in Table 1 that behave very much as we would expect our dipole to behave, then we can use the equations that describe those curves to produce reasonable estimates of the values of the antenna input impedance between the values we've calculated using the antenna modeling program. One technique that will give us such equations is the method of least squares.[8] From our observations of Figure 1, we'll elect to use a linear fit for the reactive component and a parabolic (second degree) fit for the real component.

To help us avoid a number of tedious and error-prone manual calculations, *Octave* includes a powerful curve fitting function, *polyfit*, that will give us the coefficients of the polynomials we need to fit the data we have. *Polyfit* is defined as follows:

[P, S] = polyfit(X, Y, N)

where:
P is a row vector containing the coefficients of the fitted polynomial of degree *N*.
S is a structure containing information about how the fit was obtained and the quality of the fit. We won't use *S* for the purposes of this article.
X is a row vector
Y is a row vector.
N is the degree of the polynomial fit we'd like to fit to the points in *Y* taken as functions of the points in *X*.

We let the values in *X* represent the frequencies at which we have antenna impedance calculations, and those in *Y* represent the impedance values taken one component at a time, real and imaginary.

The code in Table 3 defines the frequencies of interest as *fn* and vectors of real and imaginary components of the antenna impedance as *Rnec2c* and *Xnec2c*. When we run *polyfit* with $N = 1$ for the reactive components and $N = 2$ for the real components, we get the polynomial coefficients we will use in Table 3 to define *Rfit* and *Xfit*. Note that five discrete frequencies are stored in the vector *fn* while the function *linspace* is used to store

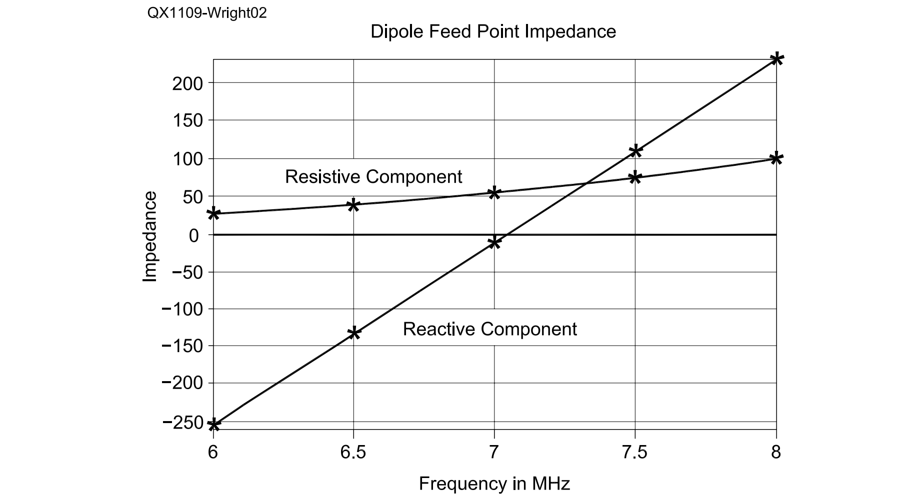

Figure 2 — Impedance of dipole from least squares curve fit.

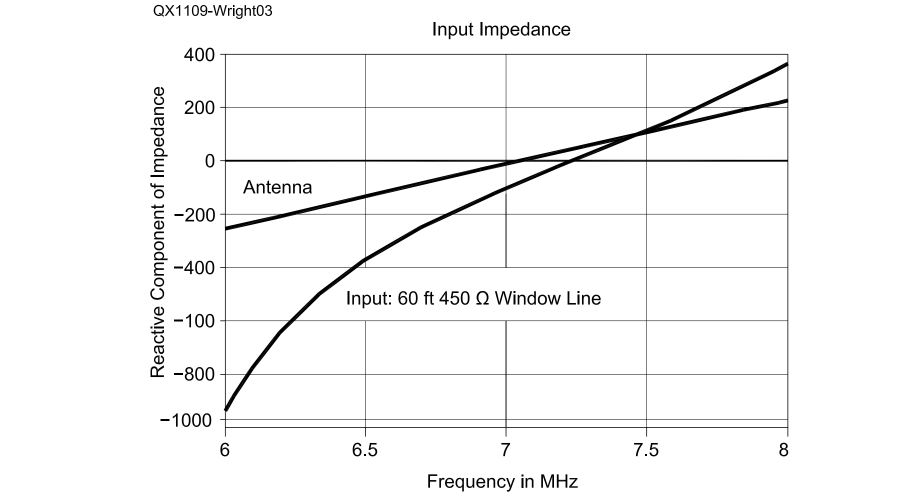

Figure 3 — Input reactance for 450 Ω transmission line terminated with a dipole.

Table 2
***Octave* Code to Plot Discrete Calculations of Antenna Reactance**

```
#! /usr/bin/octave -qf
fn = [6.0, 6.5, 7.0, 7.5, 8.0];
Rnec2c = [26.91, 38.10, 52.94, 72.47, 98.06];
Xnec2c = [-254.8, -131.0, -10.78, 108.6, 229.2];
plot(fn, Rnec2c, "-", fn, Xnec2c, "-", fn, 0 .* Xnec2c, "-");
title( "DIPOLE FEED POINT IMPEDANCE");
xlabel( "FREQUENCY IN MHz");
ylabel( "IMPEDANCE IN OHMS");
text(6.6, 70,  "RESISTIVE COMPONENT")
text(6.75, -100,  "REACTIVE COMPONENT")
grid;
pause;
```

101 values from 6.0 to 8.0 MHz in the vector *ff* so that we can approximate a continuous curve when we plot *Rfit* and *Xfit*.

At this point, we could write the following equations using the data stored in *Rcoef* and *Xcoef*:

$$Rfit = 9.5686 \times ff^2 - 98.6260 \times ff + 274.4337; \quad \text{[Eq 1]}$$

$$Xfit = 241.52 \times ff - 1702.40 \quad \text{[Eq 2]}$$

An easier, and less error prone way to form these equations, though, is to use the *Octave* function *polyval*, which is defined as follows:

S = polyval(C, X)

where:
S is a row vector containing values of *C* evaluated at the points specified in *X*.
C is a row vector containing the coefficients of the polynomial to be evaluated.
X is a row vector containing the arguments of function *C* at which we would like evaluations.

Note that these equations are typeset as mathematical expressions, but that the actual *Octave* code in Tables 2, 3 and 4 show how to create the equation in *Octave*. The *Octave* code uses a decimal point before an operator to tell *Octave* to perform element by element arithmetic rather than matrix arithmetic. "*Octave* for Transmission Lines," in the Jan/Feb 2007 issue of *QEX* included a short tutorial and some examples of the difference between the "dot operators" and their "undotted" counterparts. See Note 2.

For the purposes of our curve fit, we'll use:
Rfit = polyval(Rcoef, ff);
Xfit = polyval(Xcoef, ff);

We'll put all this together in Table 3 and run the code under *Octave* to get both the lines and stars of Figure 2. Note that the stars, representing our antenna calculations using *nec2c*, fall very close to the lines that represent our fitted curves, indicating that the two curve fits are close. If we wanted to do a more detailed mathematical analysis of the "goodness of fit," we could use the data stored by *polyfit* in *S*, but that won't be necessary here as we can see from Figure 2 that the fit is sufficient for our purposes.

Modeling the Transmission Line

Looking at Figure 2, we see that the antenna has an impedance of about 54 Ω resistive in the vicinity of 7.050 MHz, just what we were looking for. What then, went wrong? We should remember that we used the antenna analyzer at the end of 60 feet of 450 Ω transmission line, not at the antenna, and that the 450 Ω line presents quite a mismatch to the antenna even though its attenuation per unit length is low. Let's modify the code from *Octave for Transmission Lines* to look at the problem we have here. We'll include data on the load impedance using the curve fits we developed above and we'll specify the characteristics of the transmission line in the code rather than accepting it from the keyboard.

We used WM CQ 553 open wire line in our installation, so we'll pull data from Table 22-60 of *The 2011 ARRL Handbook*:
$Z_0 = 450\ \Omega$
$VF = 91\%$

f in MHz	1	10	100	1000
atten in dB / 100 feet	0.06	0.2	0.7	2.9

Z_0 and *VF* are relatively constant over a broad range of frequencies and we can enter them into our code as constants. The value for *atten*, though, varies over the range in which we are interested. Fortunately, *atten* varies rather predictably as the square root of frequency over the range of frequencies of interest to us for almost all transmission lines. We'll solve for a multiplying constant at 10 MHz and end up with:

$$atten = 0.0632 \times sqrt(f) \quad \text{[Eq 3]}$$

as we did in *Octave for Transmission Lines*. (See Note 2.)

We'll eliminate the keyboard input com-

Table 3
***Octave* Code to Plot Least Squares Fit to Antenna Reactance**

```
#! /usr/bin/octave -qf
ff = linspace(6.0, 8.0, 101);
fn = [6.0, 6.5, 7.0, 7.5, 8.0];
Rnec2c = [26.91, 38.10, 52.94, 72.47, 98.06];
Xnec2c = [-254.8, -131.0, -10.78, 108.6, 229.2];
Rfit = 9.5686 .* ff .^ 2 .- 98.6260 .* ff .+ 274.4337;
Xfit = 241.52 .* ff .- 1702.40;
plot(ff, Rfit, ff, Xfit, fn, Rnec2c,  "*", fn, Xnec2c,\
  "*", ff, 0 .* Xfit);
title( "DIPOLE FEED POINT IMPEDANCE");
xlabel( "FREQUENCY IN MHz");
ylabel( "IMPEDANCE IN OHMS");
text(6.6, 70,  "RESISTIVE COMPONENT")
text(6.75, -100,  "REACTIVE COMPONENT")
grid;
pause;
```

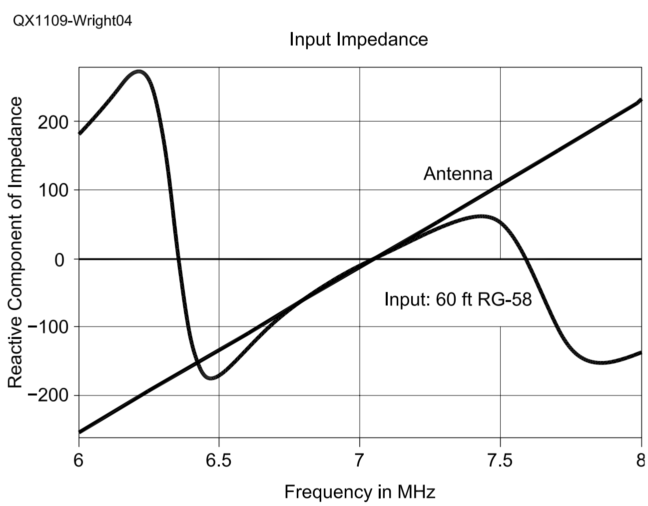

Figure 4 — Input reactance for 50 Ω transmission line terminated with a dipole.

mands from the code we're borrowing from *Octave for Transmission Lines* and embed the data in the code. We'll plot the data rather than printing it out and we'll consider only the reactive component of the input impedance to the line as we're interested in "resonance," the point at which our antenna analyzer will detect that the reactive component of impedance has passed through zero ohms. Our code is listed in Table 4.

The plot we get by running the code in Table 4 under *Octave* is shown in Figure 3. For comparison purposes, we've plotted the reactance of the antenna along with the reactance observed at the input to the transmission line and with a horizontal line to clarify the zero crossing points. Rather than transfer data manually — an error-prone procedure — we've moved our code for developing the curves from Table 3 to Table 4. We get both plots at all 101 points, approximating continuous curves.[9]

We've also added labels to the plots using the *text* command. We could instead have used *legend* to show a legend of the different curves as we have in previous articles, but *legend* works by differentiating between colors or line styles and it seems to me that this figure is most clear when both plots are represented by solid lines.

Interpreting the Results

When we examine Figure 3 we see that the 450 Ω transmission line has shifted the reactive component of impedance as a function of frequency so that the zero crossing is at about 7.23 MHz, and that's what our antenna analyzer reported as the resonant point.

Why were the 80 meter folks in operation so rapidly with no concern about their antenna? Well, they were using 50 Ω coax instead of open-wire line. The low loss of the coax on 80 meters made the inconvenience of ladder line unnecessary in their minds.

Let's see what would have happened if we had used coax on 40 meters. We'll pull the data for an RG-58 coaxial line (Belden 7807A) from Table 22-60 of *The 2011 ARRL Handbook* and we've included that data in the code in Table 4, commented out. Note that we curve fitted the attenuation data for the attenuation per unit length using the same square root of frequency model as we did for the window line. Since we'll need a different label in the plot for the coax and the locations of the labels will be different, we include extra *text* statements, now commented out, for the coax. The results are plotted in Figure 4.

Note that, since the coax is a good match to the antenna over frequencies near the antenna resonant frequency, the reactive component of impedance isn't changed much by the trip down the transmission line. As we move away from resonance, though, the reactance of the line will mismatch the increasing positive or negative reactance more severely than was the case with the 450 Ω line and the excursions away from zero reactance will be more pronounced. The analyzer told the 80 meter folks that their antenna/coax combination was resonant where they wanted it to be and they started operating immediately.

Conclusions

We've learned here to be a little careful about what an antenna analyzer tells us, especially when there is a length of transmission line between the antenna and the analyzer.

We've also learned to use a powerful toolset consisting of *Octave's* functions *polyfit* and *polyval*, along with *Octave's* ability to process large matrices or vectors of data with single operators or function calls.

Table 4
***Octave* Code to Plot Input Impedance of Transmission Line Terminated in Dipole**

```
#! /usr/bin/octave -qf
f = linspace(6.0, 8.0, 101);
fd = [6.0, 6.5, 7.0, 7.5, 8.0];
d = 60;  # length of line in feet
a = 0.0648 .* sqrt(f) .- 0.0048;    # alpha for 450 ohm line
v = 91;                             # 450 ohm open wire line
Zo = 450;                           # 450 ohm open wire line
#a = 0.3237 .* sqrt(f) .-0.02373;   # alpha for 50 ohm coax
#v = 85;                                         # 50 ohm coax
#Zo = 50;                                        # 50 ohm coax
Rd = [26.91, 38.10, 52.94, 72.47, 98.06];
Xd = [-254.8, -131.0, -10.78, 108.6, 229.2];
Rcoef = polyfit(fd, Rd, 2);
Xcoef = polyfit(fd, Xd, 1);
Rt = polyval(Rcoef, f);
Xt = polyval(Xcoef, f);
a = a ./ 1e2;  # convert dB per 100 feet to dB per foot
a = 0.1151 .* a;  # convert dB to nepers
c = 9.836e8;  # speed of light in feet per second
lambda = c ./ (1e6 .* f);  # wavelength of signal in vacuum
lambda = (v ./ 1e2) .* lambda; # adjust lambda for velocity
B = (2 .* pi) ./ lambda; # calculate Beta
Zt = Rt .+ j .* Xt;  # calculate complex terminating impedance
Zd = Zo .* tanh((a .+ j .* B) .* d .+ atanh(Zt ./ Zo));
plot(f, imag(Zd), f, Xt, f, 0 .* Xt,  "-b");
title( "INPUT IMPEDANCE");
xlabel( "FREQUENCY IN MHz");
ylabel( "REACTIVE COMPONENT OF IMPEDANCE");
text(6.2, -110,  "ANTENNA")
text(6.4, -550,  "60 FEET 450 OHM WINDOW LINE")
#text(7.4, 150,  "ANTENNA")
#text(7.4, -120,  "60 FEET RG-58")
grid;
pause;
```

The method of least squares implemented by these functions and the ability to use the coefficients of even a high order curve fit without manually transferring them allows efficient, error-free approximation of relatively complex sets of data.

Some Cautions

The method of least squares is a powerful curve fitting tool. It can, though, lead us astray if we're not careful. Let's fit a curve to a sine wave to experiment a little. We wouldn't normally need to do that, but it provides a good example for study, because we already know the nature of the curve we're trying to fit. We'll represent the sine wave by a series of points as shown in the vector *amplitude* in the *Octave* code in Table 5. Sine waves, exponentials, and other relatively complex functions may be represented by infinite series of polynomial terms, so it's possible to use a polynomial generated by a least squares fit as a truncated infinite series approximation to the infinite series that would exactly represent our sine wave.[10, 11] Using the code in Table 5, we have plotted in Figure 5 a fifth degree least squares fit to the several points in *amplitude*. We've also plotted a 101-point approximation to the sine wave and the two are so close that the traces are almost convergent at all points.

Shouldn't we get a better fit if we add more terms to the polynomial by increasing its degree? We've done that in the seventh degree fit in Table 5 and Figure 5. Note that the least squares computation doesn't "know" what we're trying to do. It "knows" only that we want a curve that passes as closely as possible to the five points we specified in the argument to *polyfit*. If we look at the seventh degree fit, we can see that it passes through all the points as closely as we can tell from the Figure, but it does so by producing a curve that wanders around a bit and doesn't look much like the curve from which we selected our five sample points.

Be cautious when curve fitting. Be familiar with at least the general shape of the curve you are expecting and, in most cases, use the lowest degree least squares fit that will accomplish your purpose.

Notes:

[1]H. Ward Silver, NØAX, Ed, T*he ARRL Handbook for Radio Communications*, *2011*, The American Radio Relay League, Inc. 2010

[2]Maynard Wright, W6PAP, "Octave for Transmission Lines," *QEX*, Jan/Feb, 2007, pp 3-8.

[3]The program *nec2c* is a port of *NEC2* from *FORTRAN to C* by Ray Anderson, WB6TPU. You can download nec2c from **www.si-list.org/swindex.html**.

[4]You can download the latest *Octave* files at **www.octave.org**.

[5]The *Octave* code presented in this article is available for download from the ARRL *QEX* files website: **www.arrl.org/qexfiles**. Look for the file **9 × 11 _Wright.zip**.

[6]Dean Straw, N6BV, Ed, *The ARRL Antenna Book*, 21st Edition, The American Radio Relay League, 2007, p 5-6.

[7]An older edition of *The ARRL Antenna Book* (13th Edition, 1974) includes a figure (Figure 2-7 on page 30) that is similar to our Figures 1 and 2, but using normalized frequencies.

[8]C. Ray Wylie, *Advanced Engineering Mathematics, Fourth Edition*, McGraw-Hill, 1975, pp 153-170.

[9]Using 101 points causes the frequencies between 6 and 8 MHz to fall directly on every other one hundredth megahertz between the two terminal frequencies. This may lead to a neater printout if we were to decide to use *printf* to print out discrete values of reactance rather than plot them.

[10]W. L. Hart, *Analytic Geometry and Calculus*, D. C. Heath and Company, 1957, pages 547-560.

[11]The fit is only an approximation to a truncated infinite series, but often a good one, as is the case with our sine wave here. The usual series expansion of a sine wave includes only odd exponents of x, while the least squares fit involves terms of all integral exponents up to argument N to polyfit, so the fit we are getting here is not exactly analogous to a truncated infinite series.

Table 5
***Octave* Code to Fit and Plot a Sine Wave**

```
#! /usr/bin/octave -qf
fn = [100, 200, 300, 400, 500];
ff = linspace(100, 500, 101);
amplitude = [0.0, 1.0, 0.0, -1.0, 0.0];
sine_coef_5 = polyfit(fn, amplitude, 5);
sine_coef_7 = polyfit(fn, amplitude, 7);
sine_fit_5 = polyval(sine_coef_5, ff);
sine_fit_7 = polyval(sine_coef_7, ff);
plot(ff, sine_fit_5, ff, sine_fit_7, ff, sin((ff .- 100) .* 2
.* pi ./ 400));
title( "LEAST SQUARES FIT TO SINE WAVE");
#xlabel( "FREQUENCY IN MHz");
#ylabel( "IMPEDANCE IN OHMS");
text(340, -0.50,  "5th DEGREE FIT")
text(405, 0.77,  "7th DEGREE FIT")
grid;
pause;
```

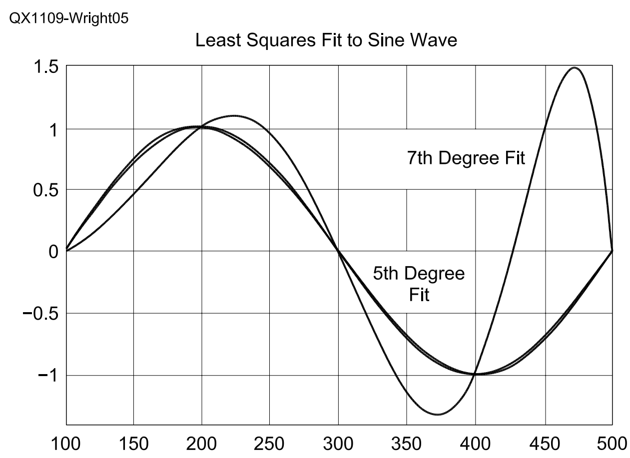

Figure 5 — Sine wave using least squares fit.

Bob Allison, WB1GCM, ARRL Test Engineer; **ballison@arrl.org**

Book Review: Receiver Design and Technology

Cornell Drentea, KW7CD
Artech House, 2010
462 pages, $149
ISBN-13 978-1-59693-309-5

Radio amateurs may be familiar with the block diagrams of various superheterodyne receiver types; single conversion, dual or more conversion, or direct conversion. Each block represents a necessary stage with its specific function; mixing, amplifying, tuning and so on. Many of us had to memorize the block diagrams, placing each stage in the proper order, to attain a higher class of Amateur Radio license. Sometimes, we forget all of it, but would like to get reacquainted.

Many years ago, I decided RF was what I wanted to study at the University of Hartford. I quickly felt quite over my head after reading my first receiver design theory book! Yes, the designs were understandable, but the text was often lacking in explanation as to "how" and "why." For instance, how do you pick the best intermediate frequency or frequencies? What makes a good mixer? I got through the course all right and continued my RF courses, going on to what I liked best at the time: transmitters. A few years ago, I became Test Engineer at the ARRL Laboratory, which includes evaluating receiver performance. Now such questions as "what makes a good mixer" is a rather interesting topic to investigate. Fortunately, I recently obtained Cornell Drentea's book, *Receiver Design and Technology*. This comprehensive and well illustrated text book is a delight to read, unlike my old college text books. Mind you, the theory *is* complex, but for anyone wishing to dig deeper into what makes a receiver work *and* work well, this book will answer all questions the reader is asking. It is quite suitable as a college text book but appropriate for the beginners and old-timers as well.

What made this book special from the very start was the preface. In it, the author tells an autobiographical short story about a nearly six year old boy who wanted to take apart his Dad's radio, "to see what the little people inside looked like." With both parents away from home and with pliers and a screwdriver in hand, little Cornell quickly had the radio totally dismantled. Unexpectedly, the parents returned early, before he was able to re-assemble the radio. This touching story (with a happy ending) reminded me of the human side of technology; it is our nature as radio amateurs to find out how it all works. The preface also gave me the feeling that a real person, someone I can relate to, is speaking to me and I am about to learn something great.

The first chapter is a brief history lesson on some of the names of the inventors and developers of radio technology. Interestingly, it also poses the question and gives a surprising answer to, "who invented radio?" I liked the fact that the author mentions, "One must not forget the many dedicated ham radio operators around the world." The following brief chapter describes the history of radio, complete with schematics, from Edouard Branly's Coherer, up to Armstrong's development of the Superheterodyne Receiver. I found the diagram of DeForrest's Audion Receiver interesting since the ARRL has one (with tube) in W1AW's foyer. While I enjoy historical topics, I also enjoy the latest technology topics. As I read through the subsequent chapters I had many eye popping experiences.

Though each chapter is very comprehensive, the mathematics used to describe the various concepts gets right to the point and is not overwhelming, as it can be in other text books. Mathematical proofs are for mathematicians, not for me. The lack of proofs leaves more space for more usable information, and this book has plenty of that.

After an introduction to the superheterodyne receiver, Chapter 4 digs into the implementation of a single conversion receiver and clearly describes the various parts in subchapters. The list of topics in succeeding chapters is too long to list here; topics that include discussions of varieties of superhetrodyne receivers, mixers, frequency synthesizers, AGC, digital signal processing, software defined radios, and warfare receivers. Crystal filter design fans will be very pleased too. An added bonus is a chapter on the Arecibo Observatory. In that chapter, the author mentions that with today's technology, useful reception of intelligent signals from a planet 15,000 light years away is possible. That would be pretty good DX.

Readers of *QEX* may be familiar with Cornell Drentea's three part series on the design and development of his high performance, home brew, Star-10 Transceiver.[1] The Star-10 transceiver was designed and built as a project with the intent of finding out what could be done to achieve ultimate performance. The author uses this exceptional HF transceiver as an example of receiver design in a few of the chapters. Some of the topography and illustrations seen in *QEX* are reproduced in *Receiver Design and Technology*. An example of this is how and why the IF frequencies are chosen. By using an Intermodulation Distortion Web Analysis Tool, the design engineer may quickly find the proper combination of frequencies that will minimize the spurious response of a mixer. The material originally from *QEX* is very useful. We are lucky to have this gentleman build this complex device from a "laws of physics" point of view, and that he is sharing all of this knowledge with us.

With Cornell Drentea's marvelous style of writing, *Receiver Design and Technology* will educate, excite, and inspire many. This text book should be used on every college campus that offers such a course. There is

[1]Cornell Drentea, KW7CD "The Star-10 Transceiver," *QEX*, Nov/Dec 2007, Mar/Apr 2008, May/Jun 2008.

a great demand for RF engineers today, and this book will undoubtedly inspire students to become engineers. While I can lament the fact that I didn't have a text book such as this one thirty years ago, I am happy to have this text book today.

Cornell Drentea is an accomplished RF technologist, an engineer and a scientist with fifty years of hands-on experience in the aerospace, telecommunications and electronics industry. He has been involved in the design and development of complex RF, radar, guidance and communications systems at frequencies up to 100 GHz. He has developed several state-of-the-art products for companies such as Honeywell and Raytheon. This includes, but is not limited to, ultra wide-band, high probability of intercept microwave receivers, complex synthesizers, and deep-space Doppler agile transceivers. He is known for his scientific and technical publications on the subject of applied RF technology. Cornell has published over 90 technical papers and articles in national and international magazines. He has been a consultant and is currently teaching comprehensive RF design courses to some of the largest international companies. He holds five patents. Cornell holds an Extra class amateur radio license KW7CD.

Bob Allison resides with his wife of 27 years, Kathy, KA1RWY, in Coventry, CT. Before coming to the American Radio Relay League as the Product Review Test Engineer in April of 2008, Bob worked at WVIT-NBC CT (Channel 30) for 28 years as an Engineer and Studio Supervisor. Bob is a graduate of Ward Technical College, finishing up his last year at the University while working full time at Channel 30 in 1982. His Hobbies are Amateur Radio (37 years), Antique Radios and enjoying his 1931 Model-A. He is also an avid sailor. Bob also volunteers as a tour guide at the Vintage Radio and Communications Museum in Windsor Connecticut.

QEX

Ray Mack, W5IFS

17060 Conway Springs Ct, Austin, TX 78717; w5ifs@arrl.net

SDR: Simplified

We resume the SDR series in this issue with a look at Cascaded Integrator Comb Filters.

The past year has been full of activities that kept me away from writing this series. That is all behind me now, so we can get back to experiments and learning about software defined radios.

Introduction to CIC Filters

We looked briefly at the theory of the sampling down converter (decimator) in the Nov/Dec 2009 issue and the sampling up converter (interpolator) in the Jan/Feb 2010 issue. An interpolator is typically used in a transmitter to increase the sample rate of a signal in preparation for frequency translation to the final frequency. A decimator is typically used in a receiver to lower the sample rate and also translate the signal to a lower frequency. In the interpolator, we add zero samples in between our existing samples and then low pass filter the sequence to eliminate images of the original. The result is a new sequence of samples that has the same spectrum as the original but with samples at a much higher rate. A decimator works similarly, but we throw away existing samples and low pass filter the sequence to eliminate unwanted aliases of higher frequencies. This new sequence also has the same spectrum (or an aliased spectrum) as the original, but with a lower sample rate.

The filter for an interpolator or a decimator can be a finite impulse response (FIR) or infinite impulse response (IIR) filter. The problem with both types of filters is that they require a large number of multiply operations, which consume a large number of DSP processor cycles. Eugene Hogenauer developed a very useful simplification of the sample conversion/filter configuration called a cascaded integrator comb (CIC) filter. He presented this design in an article in the *IEEE Transactions on Acoustics, Speech and Signal Processing* in April 1981.[1] The important aspect of CIC filters is that only addition, subtraction, and delay operations

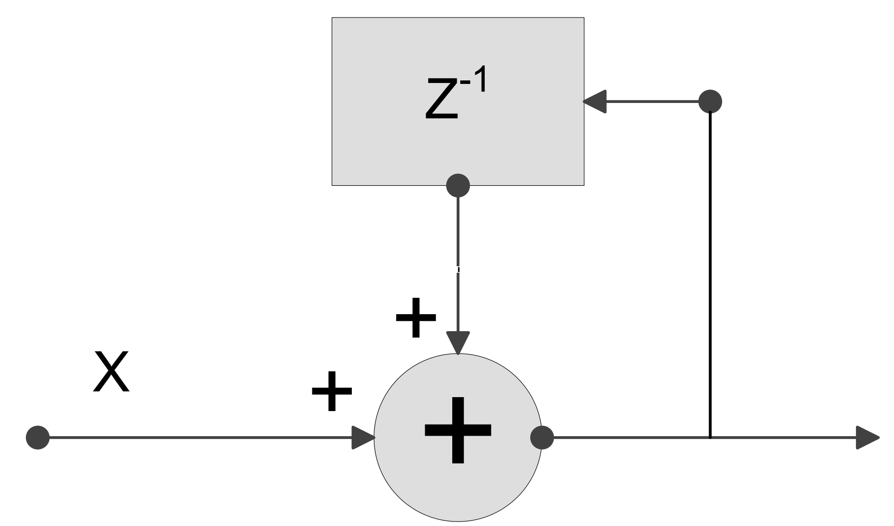

Figure 1 — Z Transform diagram of an integrator. The new output is the sum of the previous output and the new sample

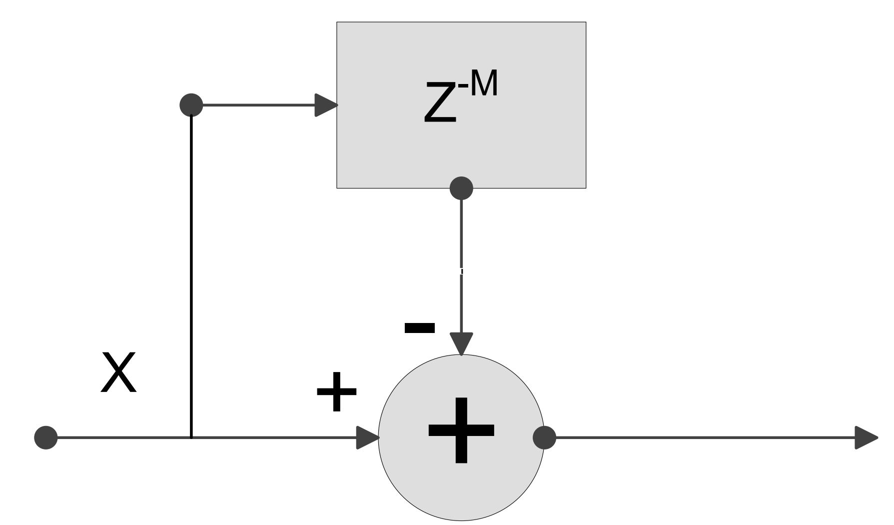

Figure 2 — Z Transform diagram of a comb. The new output is the difference of the present sample and a delayed sample. The number *M* designates how many steps happened during the delay.

[1]Notes appear on page 36.

are required for implementation.

As with most things in life, improving one aspect of a system requires compromise in other aspects. This is also true of CIC filters where we trade the simplification of eliminating multipliers for restricting the filter response. A CIC filter can only be low pass. Additionally, there is a limited subset of possible low pass responses constrained by the sample rate change and number of stages in the comb and integrator stages. The most important property of a CIC filter is that it can be very easily implemented in hardware either in an FPGA or as part of the dedicated logic of an IC such as the AD9874 and AD9957.

How a CIC Filter Works

Matthew Donadio has written a very good description on his website of how a CIC filter works, along with the associated mathematics (in case you want to see what the Z-transform equations look like).[2] I have borrowed several of his examples. We haven't used standard Z-transform graphical notation up to now, but I believe it will help you understand the framework.

The integrator is an infinite impulse response filter. Figure 1 shows how it works and how simple it is. The integrator holds a running total of all previous samples. The integrator adds the last output value (z^{-1}) to the current input value (x). Ordinarily, we would worry about overflow in an integrator because a dc component in the signal will cause the integrator to overflow. The combination of the comb and the integrator, however, cancels any problems with overflow (see Donadio for details). The integrator is a single pole low pass filter with infinite

Listing 1
GnuPlot

```
R=8
N=4
M=1

set angles radians
#set the grid lines to dots
set grid linetype 13, linetype 13
#turn on the x and y tic marks
set grid mxtics
set grid mytics
#set the intervals for major and minor grids
set xtics 0.05
set mxtics 2
set mytics 5
#set a large number of samples to create a smooth plot
set samples 100000
#set the x axis to span fs*-0.125 to fs*0.5
set xrange [-0.125:0.5]
#set the y span from -80dB to 0 dB
set yrange [-80:0]
set ylabel "dB"
Set xlabel "Frequency (f/fs)"
sinc(x) = (sin(3.14 * x * R))/(sin(3.14 * x))
CIC(x) = abs(sinc(x))
db_response(x) = (20 * log10 ( (CIC(x)**N)/(R**N) ) )
plot db_response(x) with lines 1
```

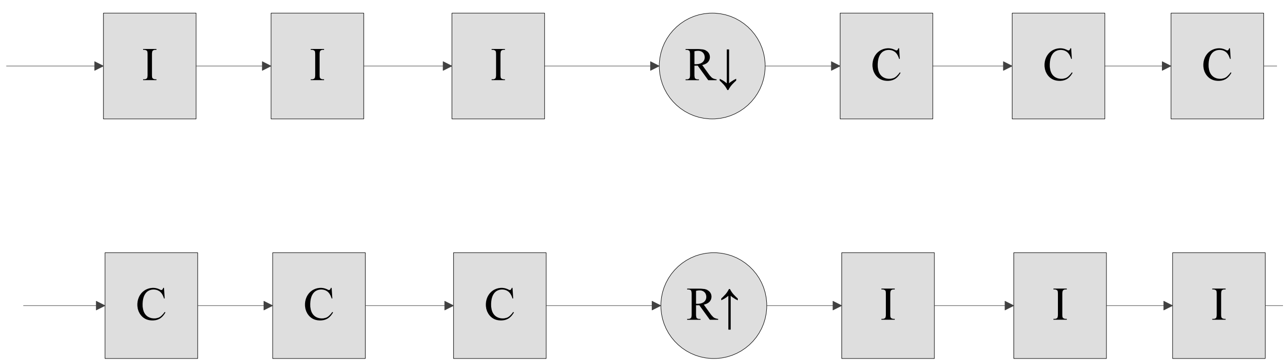

Figure 3 — The top diagram shows a decimator, where the sample rate is reduced by a value "*R*." The bottom diagram shows an interpolator where the sample rate is increased by a value "*R*." Note that the difference between the two is the order of the combs and integrators as well as the direction of the rate change. The combs are on the low sample rate side of both systems.

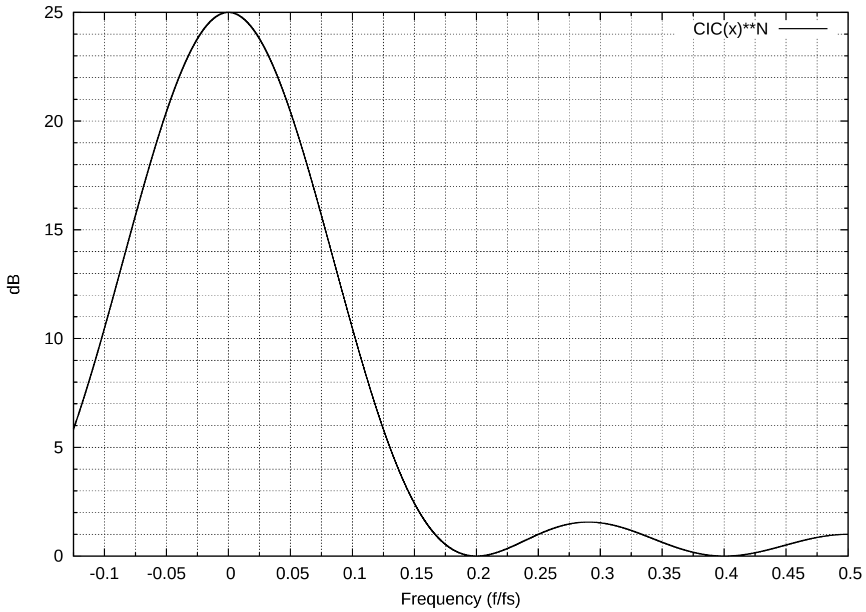

Figure 4 — The sin x/x shape of a CIC filter. The lobes decrease quickly because the sin x/x function is raised to a power.

Listing 2
C Program CIC filter

```
int accumulator_1, accumulator_2, accumulator_3, sample;
int comb_1_out, comb_1_delay;
int comb_2_out, comb_2_delay;
int comb_3_out, comb_3_delay;
#define RATE_CHANGE   9  // 1 + desired rate change

int integrator (int new_sample, int integrator_accumulator)
{
  return (accumulator + new_sample);
}
int main(void)
{
int i;
  i = 0;
  while (1)
  {
    sample = read_adc();
    // do the accumulation in reverse order so it ripples
    // in the correct way
    accumulator_3 = integrator(accumulator_2, accumulator_3);
    accumulator_2 = integrator(accumulator_1, accumulator_2);
    accumulator_1 = integrator(sample, accumulator_1);
    if ((i % RATE_CHANGE) == 0)
    {
      comb_3_out = comb_2_out - comb_3_delay;
      comb_2_out = comb_1_out - comb_2_delay;
      comb_1_out = accumulator_3 - comb_1_delay;
      comb_1_delay = accumulator_3;
      comb_2_delay = comb_1_out;
      comb_3_delay = comb_2_out;
      write_output_dac(comb_3_out);
      i = 0;
    }
    i++;
  }
}
```

gain at dc. Hogenauer figured out that the system doesn't care about overflow as long as the integrators are implemented with adders using two's complement addition that allow wrap around when overflow occurs, and that the number of bits in the word is as big as the expected output word.

[Wikipedia tells us that "the two's complement of a binary number is defined as the value obtained by subtracting the number from a large power of two (specifically, from 2^N for an N-bit two's complement). The two's complement of the number then behaves like the negative of the original number in most arithmetic, and it can coexist with positive numbers in a natural way." — *Ed.*][3]

The comb is a finite impulse response stage that subtracts a previous sample from the present sample. The amount of delay between the present sample and the delayed sample is called the differential delay and is denoted as M by most authors. Figure 2 shows the operation of the comb. A real implementation of a CIC filter is composed of multiple integrator-comb sections that are cascaded. A CIC filter has exactly the same number of integrators as combs. Remember the associative property of math from elementary school: you can rearrange the order of the additions in a sequence and the result of the sequence does not change $(a + (-b) + c + d + (-e) + (-f)$ is identical to $a + c + d - b - e - f)$. A CIC filter with rate change uses that property to group all of the integrators together and to group all of the combs together. We place either a down sample or up sample rate changer between the combs and integrators. Figure 3 shows that a decimator is an integrator section followed by a down rate change, which is then followed by a comb section. An interpolator turns the system around and puts the comb section first, followed by an up rate changer, which is followed by an integrator section. It is very useful for a hardware implementation that the number of integrators and combs is independent (within reason) from the rate change and that, in general, you can rearrange the inputs, outputs, and rate change to create a decimator and interpolator with the same blocks.

Richard Lyons has a third way of explaining the operation of a CIC filter.[4] Unfortunately, Lyons, Donadio, and Hogenauer do not do a really good job of connecting the relationship between the rate change and the differential delay in the comb. Lyons comes closest when he describes the sinc shape in terms of the differential delay in the comb section. What he did not explicitly say is that the sinc shape of a combined comb and integrator is the product of the rate change (R) and M. Both Donadio and Lyons express the number of nulls in the CIC response as a function of the differential delay, M, but they leave out the very important requirement that it applies when R = 1 (no rate increase or decrease). A normal implementation places the rate change ahead of the comb, so the effect is to transfer the number of nulls from M to R. When we add a rate change, we swap the values, so R has a value greater than one and M = 1.

Implementation Details

There are three parameters that affect the implementation of a CIC filter. "R" is the up sample rate or down sample rate. "M" is the delay in the comb section and is almost always either one or two. "N" is the number of stages in the comb section (which is required to be the same as the number of integrator sections). The simplification of separating the combs into one section and the integrators into a second section is advantageous for the speed required of the storage elements for the combs. The combs always operate at the low frequency end of the system and the integrators work at the high speed side of the system.

Notice that the associative property would also allow a decimator with the comb first and the integrator after the down converter. Either configuration will give the same results. The reason we always put the comb on the low sample rate side of the system is pragmatic. The comb requires one additional storage element (for the usual M = 1 situation) over what is required for an integrator. Each storage element consumes power when it is clocked. A faster clock and more storage registers translate directly into additional power dissipation. The additional power is an issue when implementing a CIC filter in hardware such as an FPGA.

Figure 4 shows the (sin x) / x (also called the sinc function) shape of the frequency response of a CIC filter. The full equation is:

$$H(f)=\left[\frac{\sin \pi M f}{\sin \frac{\pi f}{R}}\right]^N \qquad \text{[Eq 1]}$$

If x is very small, then sin(x) is approximately x. When R is a large value the denominator becomes $\pi f / R$ so you can approximate the shape of the frequency response in the first region (with the help of a lot of Algebra) as:

$$H(f)=\left[RM\frac{\sin \pi RMf}{\pi RMf}\right]^N \qquad \text{[Eq 2]}$$

The frequency response has nulls when f is equal to a multiple of 1 / RM. We looked in detail at the sinc function when studying the frequency response of a real world DAC (Jan/Feb 2010 *QEX*). A CIC filter suffers from the same frequency droop issue when the output bandwidth is substantial compared to the output sample frequency. Another important characteristic of the CIC filter is that the aliases for decimation and images for interpolation occur centered on the nulls of the response. Figure 5 shows a representation of the response of a decimator with R = 8, M = 1 and N = 4, where the original data is sampled at 48 kHz and the desired bandwidth is 1.2 kHz. The shading shows both the baseband energy as well as a non-trivial amount of energy in the higher frequencies that is aliased into the base band

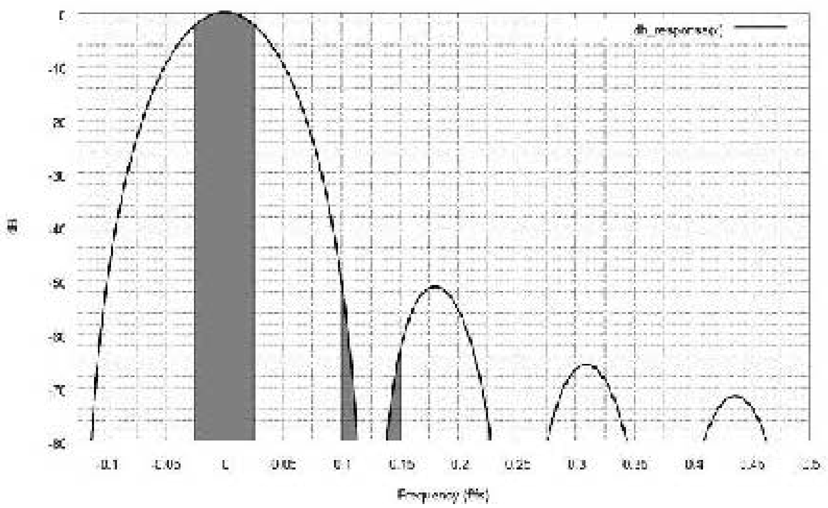

Figure 5 — The response of a CIC decimator filter with R = 8, M = 1, and N = 4. The shaded areas show the energy in the input spectrum that is included in the output of the filter.

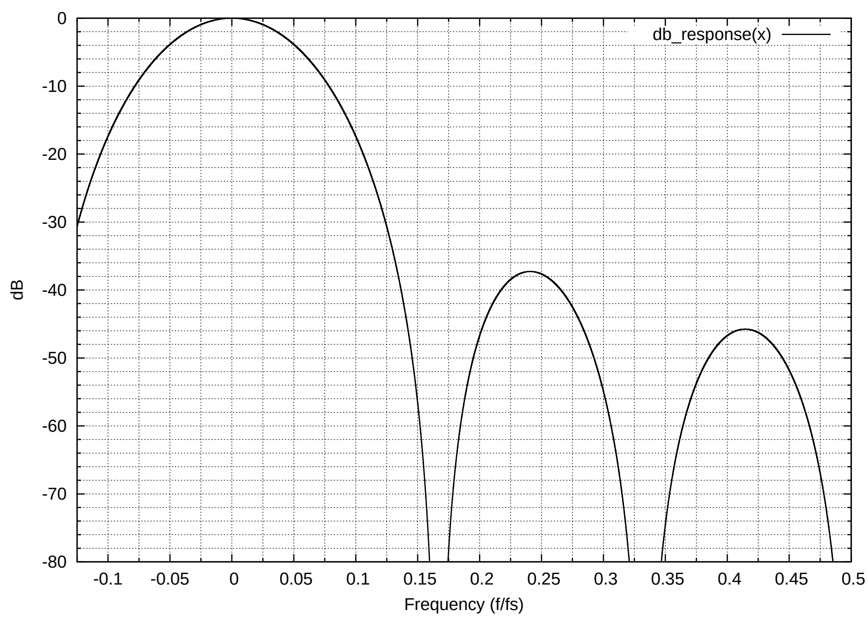

Figure 6 — The response of a CIC decimator filter with R = 6, M = 1, and N = 3. The droop is less in this filter, but alias energy is larger by 10 dB.

and contributes to noise in the system. The alias energy in the first Nyquist zone is down only 52 dB at 1.2 kHz. The baseband energy has 2 dB of droop over the pass band. Figure 6 shows a different filter where R = 6 and N = 3. Here we see that lowering N and R has improved the amount of droop to only 1 dB and the alias energy only occupies three Nyquist zones. The alias energy in the first Nyquist zone at 1.2 kHz is only down about 42 dB, however. Listing 1 is a *Gnuplot* program that will plot the normalized response of a CIC filter. It was used to create Figures 5 and 6.

The solution to the droop issue is to implement a combination system where the initial rate conversion is aggressive, followed by an FIR droop compensation filter. The compensation filter should have a shape that is the inverse of the sinc shape over the desired baseband frequencies. In our example of a 48 kHz sampled signal that has been reduced by a factor of 8 to a 6 kHz sampled signal, we would want an FIR that increases response up to perhaps 3 kHz to compensate for the droop.

The last issue is bit growth that results from the filter gain. The gain is $(RM)^N$ from Equation 2. The number of bits required at the output of the CIC filter is:

$$B_{OUT} = N \log2 RM + B_{IN}$$

where B_{OUT} is the number of bits in each output word and B_{in} is the number of input bits. Each integrator and comb section will require B_{OUT} bits in order to avoid the problem with overflow in the integrator sections. The bit growth is not likely to be an issue for a DSP processor which will likely have 32 bit registers. It can be a problem for FPGA based systems, however. The integrators and combs need to be built with enough bits to handle the largest combination of sections and rate change. Once such a system is built, though, any rate change below that maximum will be accommodated by the design.

Listing 2 shows a *C* program that implements a rudimentary CIC filter in software on a DSP chip. Read_adc() and write_dac() are left as exercises for the reader. Code very similar to that shown could be used to implement an FPGA version, which uses a VHDL compiler.

Notes

[1]E. B. Hogenauer, “An Economical Class of Digital Filters For Decimation and Interpolation,” *IEEE Transactions on Acoustics, Speech and Signal Processing*, Volume 29, April 1981 pp:155-162.

[2]Matthew P. Donadio, “CIC Filter Introduction”, 18 July 2000, **dspguru.com/dsp/tutorials/cic-filter-introduction**.

[3]See the Wikipedia entry at **http://en.wikipedia.org/wiki/Two’s_complement**.

[4]Richard Lyons, “Understanding Cascaded Integrator-Comb Filters,” *EE Times*, March 31, 2005.

Letters to the Editor

Octave for L-Networks (Mar/Apr 2011)

Hi Larry,

Patrick Wintheiser, WØOPW, called to my attention an error in "Octave for L-Networks" in the March/April, 2011 issue of *QEX*. The sentence that reads "That will happen when the quantity under the radical in Equation 2 is negative" just above Equation 4 on page 45 should read "That will happen when the quantity under the radical in Equation 3 is negative."

I apologize for the error.

— 73, Maynard Wright, W6PAP, 6930 Enright Dr, Citrus Heights, CA, 95621; **w6pap@arrl.net**

Hi Maynard,

Thanks for sharing the text correction with us. I hope this was not too confusing to our readers.

— 73, Larry Wolfgang, WR1B, QEX Editor; **lwolfgang@arrl.org**

A Flexible 2-Port Network Calculator Tool", May/Jun 2011

Dear Larry,

Thanks to Tom McDermott, N5EG, for an outstanding article and an equally fine piece of software. I would like to make your readers aware of an alternative for recompiling the *C#* source code besides the Microsoft Express package. *SharpDevelop* is an open source package that is free. It's available at **www.icsharpcode.net/OpenSource/SD/Download/#SharpDevelop4x**.

— 73, Bruce Raymond, ND8I, 3494 Fairwood Dr, Beavercreek, OH 45432; **bruce@raymondtech.net**

Hi Bruce,

Thanks for the nice email. I've never heard of the *SharpDevelop* package. Maybe you or another *QEX* reader can tell us a bit more about this compiler and how well it works on this application.

— 73, Tom McDermot, N5EG, 3950 Southview Ter, Medford, OR 97504; **n5eg@tapr.org**

On Determining Loop Gain Through Circuit Simulation (Mar/Apr 2011)

Regarding the article by John E. Post: There are two more recent methods for loop gain simulation that improve on Middlebrook's original method from 1975 that is described in the article. You can find details on my website: **http://sites.google.com/site/frankwiedmann/loopgain**.

— 73, Frank Wiedmann, DL6SDD; **frank.wiedmann@web.de**

Dear Frank,

More sophisticated techniques than Middlebrook's original method have been developed. It isn't apparent, however, that this additional complexity provides any better results for simple low-frequency oscillators than what I presented in the article.

Thanks for sharing the information on your website.

— 73, John Post,KA5GSQ, Embry-Riddle Aeronautical University, 3700 Willow Creek Rd, Prescott, AZ, 86301; **postj@erau.edu**

Converting a Vintage 5 MHz Frequency Standard to 10 MHz With a Low Spurious Frequency Doubler (Mar/Apr 2011)

John

I read your article about adding a doubler to a vintage frequency standard, and your curiosity about the frequency dividers. I would bet that they are Miller regenerative dividers, since these were fairly common just before the digital age.

A scale of 5 divider would consist of a mixer and a pair of cascaded doublers. A scale of 10 divider would consist of a mixer and a pair of cascaded triplers. As an example, consider the scale of 10 circuit. Here is how it works. Assume the circuit is producing a 100 kHz signal from a 1 MHz input. Feed the output into cascaded triplers, giving 900 kHz. Feed the 1 MHz input and the 900 kHz signal from the triplers into a mixer. Filter the output and you have a 100 kHz sine wave. The 100 kHz signal is then fed into the triplers.

Yes, it works. Getting it to start is a little tricky. The triplers must produce some output at very low input, so Class C triplers can't be used.

I looked all over the Internet, but I couldn't find much about regenerative dividers, except at microwaves, where they are still used. Here is one web site with a brief description. **www.tpub.com/content/armymunitions/Mm03236/Mm032360045.htm.**

Hit the link labeled "Back" at the top of the page to go to the schematic.

There is also a brief discussion in *Electronic and Radio Engineering,* by F. E. Terman, 4th Edition, 1955, p 663.

I hope this is helpful. I'm curious to know what others think about this question.

— 73, David Doan, KC6YSO, 4374 Logrono Dr, San Diego, CA, 92115-5622; **david@invisible-mage.com**

Letters to the Editor (May/Jun 2010)

On page 48 of the May/June 2010 issue of *QEX*, Rod Green, VK6KRG, has a question for *QEX* readers: "I have been using a balanced mixer with the Fairchild quad switch type FST3125 IC in a direct conversion receiver. It consists of four FETs, which simply act as four SPST switches. I have used these in direct conversion receivers and at the lower frequencies — say below 20 MHz — they work very well. From about 25 to 30 MHz, however, they introduce weak drifting birdies and other noise into the audio."

My thanks to Rod for pointing out this limitation of FET switch mixers. I will keep it in mind in future receiver projects.

I suspect that the FETs are indulging in low-level UHF parasitic oscillations. The oscillations vary in frequency as the source inductance of the FET varies with instantaneous FET operating point. Remember, switches spend their switching times in their active regions.

FETs and bipolar transistors exhibit transconductance, which decreases as the frequency increases. This makes the impedance looking into the source or emitter inductive. Combined with stray capacitance, we have a tuned circuit.

Try parasitic suppressors as used in vacuum-tube transmitters: A small resistance (with or without a UHF coil in parallel, to load the UHF resonance) in series with each FET lead. Also try a ferrite bead in series with each FET lead (this places a UHF loss in series with the lead).

The oscillations might be in the drivers inside the FST3125 rather than in the FETs themselves, in which case there is not much one can do, except to use discrete FETs driven through transformers.

Modern small-geometry devices have gain at frequencies far above the frequency of intended use. If it has an active device, it can probably oscillate at VHF or UHF. Thus, *all* modern analog circuits must be built to UHF construction practices.

For example, the TIP-120 NPN and TIP-125 PNP power Darlington transistors are rated with a cutoff frequency of 1 MHz. I used some first-generation devices as audio complementary emitter followers thirty years ago on a two-sided circuit board, and they were stable. A decade later, new-production devices were much faster than the originals (though the data sheet had not changed). The same circuit and same circuit board now exhibited 50 MHz parasitic oscillations!

— 73, Peter Traneus Anderson, KC1HR, 42 River St, Andover, MA, 01810-5908; **traneus@verizon.net**

The "True" TLT H-Mode Mixer (Jul/Aug 2010)

Dear Larry

I read the article by Oleg Skydan, UR3IQO, in the July/August 2010 issue of *QEX* with great interest. His article is excellent.

By reading the text I noticed that he has concentrated on creating the best *broadband* high level mixer using Guanella and Ruthroff type transformers with FST3125 switches.

Beginning in 2005 I was similarly designing a single balanced narrow bandwidth mixer using four BS170 FETs. Each switch consisted two FETs in "antiseries" configuration. The gates and sources of the transistors were connected together, with one drain to ground and one to the transformer. The reason for this is the unavoidable output parallel diode inside each FET. During that work I recognized that the ON-state linearity of the switch was not a problem, but the OFF-state voltage handling came to be the limiting factor for increasing signal levels.

In the traditional three-winding transformer type mixer, the input voltage level doubles across the open switch, making that the unwanted limit to the allowed input level. Looking for other transformer solutions I came to the solution with a Guanella balun and a two-winding bifilar transformer and step up transformer for 50 Ω output, similar to Oleg's solution. My solution was published in *RADIOAMATÖÖRI* numbers 3 and 4, 2005. With the indicated FET switches the third order intercept with the three-winding transformer in the narrowband solution was 37 dBm and with the new type transformers it was 42.5 dBm. That is nearly a 6 dB improvement.

To conclude: The Guanella and Ruthroff solution is better, not only because of the missing open lines for broadbandedness, but also for having the capability to handle greater input levels using the same FET switches.

— 73, Jukka Vermasvuori, OH2GF, Viputie 3, 01640 Vantaa, Finland; **jukka.vermasvuori@luukku.com**

An RF Phase Meter (Nov/Dec 2010)

Hi Larry,

The RF phase meter article by Dave Bowker, K1FK, describes a useful instrument. It only gives an absolute phase difference from 0° to 180°, however, and, as the author concedes, you have to determine which phase leads the other independently. By adding a divide-by-two flip-flop between the outputs of the two comparators and the inputs to the NOR gate, the range will go from 0° to 360°, thus removing the ambiguity.

— Regards, Jim Koehler, VE5FP, 2258 June Rd, Courtenay, BC V9J 1X9, Canada; **jark@shaw.ca**

A Study of Tall Verticals (May/June 2011)

Dear Larry,

End fed half wave antennas in general and verticals in particular have been my favorite for combating ground losses for half a century now, so seeing a figure of 33% efficiency for a half wave vertical and 41.2 % for a quarter wave vertical in "A Study of Tall Verticals" by Al Christman, K3LC. caught my attention. On the surface this might be taken as a proof to the effect that a quarter wave is 25 % more efficient than a half wave, but in all fairness to the author that is not what he set out to investigate. Just comparison would involve using the same band for both antennas or else scale the ground conductivity accordingly. If that is done I guess the half wave antenna will improve its share, and it will save cost and labor for an extensive ground system.

It is important to note that the definition of efficiency used in the article is at variance with a long standing practice, as exemplified by the low values quoted. Commonly defined as the ratio between radiated power and input power to the antenna, efficiency is frequently written as

$$\eta = \frac{R_{rad}}{R_{rad} + R_{loss}}$$

The radiation resistance of a quarter wave vertical over a decent ground is known to be close to the 36 Ω value reported for the total resistance at 160 m in Table 1, showing that the efficiency of the 1,8 MHz quarter wave vertical must be near 100 %. The quoted efficiency of 41%, normally suggesting a feed point resistance approaching 90 Ω, just has to be differently defined.

The loss resistance is responsible for all power not leaving the antenna in the form of an electromagnetic wave, confining its origin broadly to the near field region. Any loss mechanism sufficiently far removed to have negligible effect on R_{loss} is not a property of the antenna according to the equation above, but belongs instead to the propagation path. Thus it is only to be expected that the article blames the lower efficiency quoted for the half wave on ground resistivity between the radials, in line with the classical definition of efficiency. The same definition shows the efficiency of the radial system employed to be excellent for the quarter wave and the half wave is known to depend less on it. So this may be a good example of how mixing two definitions of efficiency may lead us astray. What is the new definition used by the author?

Although not explicitly stated, this low efficiency is probable taken as the so called "Average Gain" of the 3-D plot in *EZNEC*. It is found by integrating the far field power density from the antenna over the half hemisphere above planar earth. The catch, however, is the fact that the method for calculating the field strength is the one used for sky-wave, a superposition of direct and ground-reflected waves. Only for the case of perfect ground does the solution using this method merge with the accepted solution for ground wave. With imperfect ground, it predicts no radiation at all along the surface due to phase reversal of reflection below the Brewster angle. The power that goes into ground wave radiation is thus effectively neglected by this method, depending on ground conductivity. The missing slice, compared to perfect ground, between the bottom of the lobes and ground in Figure 2 results in reduced input to the "Average Gain." The "thickness" of this slice is chiefly governed by reflection far from the antenna and is generally accepted as a property of the ground in the area.

The front of the lobe, at the peak gain angle, is significantly retarded by imperfect ground reflection in most cases. The loss may approach 6 dB if the angle coincides with the Brewster angle. The upper part of the lobe, representing high angle reflection, is less affected by the Brewster dip and gains increasingly from ground improvement within practical radial range as the take off angle approaches 90°. Still, an extension of radials beyond what markedly affects R_{loss} is not an improvement of the antenna efficiency according to the classical definition.

We may now visualize an alternative explanation of the somewhat disappointingly low figure of 33% quoted for the half wave antenna: Its higher directivity, compared to the quarter wave, concentrates a greater part of the radiation into the Brewster dip and the missing ground wave slice, resulting in dissipation that is mostly outside the practical limits of the antenna site and beyond significant R_{loss} effect. The confirmation offered in the article is no less valid for this explanation than the intended one, but then again one should also remember the unfair use of ground in favor of the quarter wave.

I am a recent subscriber to *QEX* and don't know if this new definition of efficiency has been gaining ground here, but I understand how it may be of interest to those who are primarily concerned with sky wave. To reduce the risk of confusion one might perhaps term it "sky wave efficiency," remembering that it is not merely a property of the antenna alone but the whole area? Or shall we just stick to Roy Lewallen's "Average Gain"?

— 73, Villi Kjartansson, TF3DX; **villik@hi.is**

Dear Villi,

You are correct. In the *QEX* article, the number I quoted for the "efficiency" of each antenna was derived simply by manipulating the value of "average" gain, which is generated by *EZNEC* whenever a 3-D plot is requested. I discussed the shortcomings of this method in some detail in an earlier article ("Ground Constants and their Impact on Vertical Monopole Performance") which was published in the March/April 2009 issue of *NCJ*. I completely omitted that material from the *QEX* article, however. Here is an excerpt from the *NCJ* article mentioned above:

"Note that *EZNEC* calculates the average gain of the antenna in the far field, at a distance that is essentially infinite. Thus, all of the power dissipated in the lossy earth is included, from the base of the vertical monopole out to an infinite distance. Further, any input power radiated as the ground-wave component of the total field is ignored when calculating average gain. As a result, the values given here for average gain and efficiency are essentially based upon the skywave portion of the total radiated fields of the antenna."

As you suggested, I should have used the term "Sky wave Efficiency" rather than "Efficiency" alone, to provide more clarity in the *QEX* article. My apologies for the omission.

— Sincerely, Al Christman, K3LC, Grove City College, 100 Campus Dr, Grove City, PA 16127.

A New Theory For the Self Resonance, Inductance and Loss of Single Layer Coils (May/June 2011)

Dear Larry,

With regard to my May/June *QEX* article, in Equations 13, 14 and 32, the term (l + δ) does not make clear that the length l is that of the wire. Also it is not consistent with my definition of δ. So (l + δ) needs to be changed to lw'. Then Equation 13 becomes:

$$f_r^{1.25} \approx [300 \times 0.5 / l_w'] / [D^2 / (73\ p)]^{0.25} \text{ MHz} \quad \text{[Eq 13]}$$

where $l_w' = l_w\,(1 + \delta)$

Equations 14 and 32 are changed similarly.

I apologize to the readers for my mistakes.

— 73, Alan Payne, G3RBJ, Laurel Bank, Sand Rd, Wedmore BS28 4BZ, Great Britain; **paynealpayne@aol.com**

Upcoming Conferences

Microwave Update 2011 and 37th Eastern VHF/UHF Conference Joint Conference Announcement

October 13-15, 2011
Holiday Inn, Enfield, CT USA

Microwave Update 2011 and the 37th Eastern VHF/UHF Conference, both Sponsored by the North East Weak Signal Group.

This year the premier microwave Amateur Radio conference and the Eastern VHF/UHF conference will include tours, hospitality, swap session, equipment for measuring and tweaking, banquet and of course technical presentations.

The Conference will be held at the Holiday Inn (formerly Crowne Plaza) Hotel in Enfield, CT. A block of rooms has been reserved at the discount price of $99/night, you must mention Microwave Update to receive discount. If you register on-line use the group code **"N09"** which allows 2 double beds, nonsmoking at a $99 per night rate. Hotel phone is 860-741-2211.

This is the same location where the Eastern VHF/UHF Conference has been held for the past 10 years. For map, directions and links to the hotel / travel accommodations see **www.microwaveupdate.org/**. There will be both a written and CD joint *Proceedings*.

Thursday Oct 13, 2011

AM - Haystack Observatory Tour - confirmed

PM - TBD

Dinner on your own

6:00 PM - 11:00 PM - Hospitality Suite

Friday Oct 14, 2011

AM - Registration, Introductions, Speakers , Auction

Lunch

PM – Demonstrations, Indoor Swap

Dinner on your own

6:00 PM - 11:00 PM - Hospitality Suite

Saturday Oct 15, 2011

AM – Registration, Introductions, Speakers, Auction, Demonstrations, Vendor Displays.

PM - Test Lab to 50 GHz, Introduction to Microwaves, Band Sessions

Evening – Banquet, Trivia Quiz, Door Prizes

Sunday Oct 16, 2011

8:00 - 12:00 Noon - Outdoor Flea Market, rear parking lot

Please visit **www.microwaveupdate.org/** for the latest updates and registration.

The 30th Annual ARRL and TAPR Digital Communications Conference

September 16-18, 2011
Four Points by Sheraton BWI Airport
7032 Elm Road
Baltimore, Maryland 21240

We hope to see you at the 30th Annual ARRL and TAPR Digital Communications Conference to be held September 16-18, 2011, in Baltimore, MD. The conference location is the Four Points by Sheraton BWI Airport, Baltimore, MD.

We recommended that you book your room prior to arriving. To book your room, use the link on the TAPR website under Conferences (**www.tapr.org/dcc.htm**) or call the hotel directly (Reservations: 1-800-368-7764, 1-410-859-3300).

The ARRL and TAPR Digital Communications Conference is an international forum for radio amateurs to meet, publish their work, and present new ideas and techniques. Presenters and attendees will have the opportunity to exchange ideas and learn about recent hardware and software advances, theories, experimental results, and practical applications.

Topics include, but are not limited to: Software defined radio (SDR), digital voice (D-Star, P25, WinDRM, FDMDV, G4GUO), digital satellite communications, Global Position System (GPS), precision timing, Automatic Position Reporting System® (APRS), short messaging (a mode of APRS), Digital Signal Processing (DSP), HF digital modes, Internet interoperability with Amateur Radio networks, spread spectrum, IEEE 802.11 and other Part 15 license-exempt systems adaptable for Amateur Radio, using TCP/IP networking over Amateur Radio, mesh and peer to peer wireless networking, emergency and Homeland Defense backup digital communications, using Linux in Amateur Radio, updates on AX.25 and other wireless networking protocols and any topics that advance the Amateur Radio art.

This is a three-Day Conference (Friday, Saturday, Sunday). Technical and introductory sessions will be presented all day Friday and Saturday.

Join others at the conference for a Friday evening social get together. A Saturday evening banquet features an invited speaker and concludes with award presentations and prize drawings.

The ever-popular Sunday Seminar focuses on a topic and provides an in-depth four-hour presentation by an expert in the field. Check the TAPR website for more information: **www.tapr.org**.

AMSAT 2011 Space Symposium and Annual Meeting

November 4-6, 2011
Wyndham Hotel
1350 North 1st St
San Jose, CA 95112
Telephone 1-408-453-6200

This year AMSAT has selected the Windham San Jose hotel for the Space Symposium. There is a free shuttle bus from the San Jose International Airport to the hotel. The Windham San Jose is located in the heart of the Silicon Valley, at the crossroads where high tech meets spectacular entertainment, less than one mile from San Jose International Airport.

The hotel rate is $79 per night plus taxes. Making reservations online use 1031FSJAM for the discount Group code. Calling the hotel directly, use Block code AMSAT for the discount.

Airport Information: San Jose International Airport is the closest to the Windham San Jose Hotel. Complimentary shuttle service to and from the airport is available by Wyndham San Jose. Shuttle service to and from Oakland International Airport or San Francisco International Airport is provided by select vendor referral. Transportation Costs (One Way): Shuttle $28 - $35 booked online thru vendor or $50 - $55 via phoned reservations. Contact the hotel for more information.

Getting there by car: The hotel address is 1350 North 1st Street, San Jose, CA 95112. A map and directions are included on the hotel website.

For more information on the hotel and to book a room, see their website at **www.wyndham.com/hotels/SJCAP/main.wnt**.

Symposium Information:

• Space Symposium with Amateur Satellite Presentations

• Operating Techniques, News and Plans from the Amateur Satellite World

• Board of Directors Meeting open to all AMSAT members

• Meet Board Members and Officers

• Annual General Membership Meeting

• Annual Banquet — Keynote Speaker and Door Prizes

The call for papers is not yet available, so please check the AMSAT website for the latest information: **www.amsat.org**. Mark your calendars now to attend this year's AMSAT Space Symposium

QEX